Phytochemistry 235 (2025) 114460

Contents lists available at ScienceDirect

Phytochemistry

journal homepage: www.elsevier.com/locate/phytochem

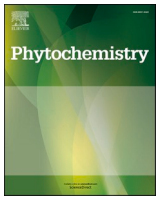

Crotoscheffleriolides, *ent*-clerodane diterpenoids from Kenyan *Croton scheffleri*

Mona Diri [a,b], Moses K. Langat [b], Eduard Mas-Claret [b], Thomas A.K. Prescott [b], Cristina D. Cruz [c], Päivi Tammela [c], Sianne Schwikkard [a,*]

[a] School of Life Sciences, Pharmacy and Chemistry, Kingston University, London, KT1 2EE, United Kingdom
[b] Royal Botanic Gardens, Kew Green, Kew, Richmond, Surrey, TW9 3AE, United Kingdom
[c] Drug Research Program, Division of Pharmaceutical Biosciences, Faculty of Pharmacy, University of Helsinki, Viikinkaari 5E, 00790, Helsinki, Finland

ARTICLE INFO

Keywords:
Croton scheffleri
Euphorbiaceae
Clerodane diterpenoids
Sesquiterpenoids
Fibroblast cell proliferation

ABSTRACT

Kenyan *Croton scheffleri* has yielded nineteen compounds. The stem bark gave six undescribed *ent*-clerodane diterpenoids (**1**–**4**, **6** and **7**), three undescribed sesquiterpene lactones (**9**, **11** and **12**) and four known compounds (**5**, **8**, **10** and **13**). From the leaves six known compounds were identified, ayanin (**14**), pheophytin a (**15**), ferulic acid (**16**), 1,3,4-trihydroxybenzene (**17**), sitosterol (**18**), and podosterol (**19**). The structures of the compounds were determined using spectroscopic and spectrometric methods, NMR, IR, UV, polarimetry, ECD, HRESIMS, and GC-MS. The undescribed compounds were assessed against HIV-1 Reverse Transcriptase and both gram-positive bacteria *Staphylococcus aureus* 29213 and *Enterococcus faecalis* 29212, as well as gram-negative bacteria *Escherichia coli* 25922 and *Pseudomonas aeruginosa* 27853. Compounds **1**, **4**, **5**, **6**, **7**, **10**, **12** and **19** increased the proliferation of serum starved dermal fibroblast cells at a concentration of 100 nM. All compounds inhibited human dermal fibroblast cell proliferation at 100 μM, while compounds **1**, **4** and **19** inhibited fibroblast proliferation at 10 μM.

1. Introduction

As part of continued study on the chemistry and pharmacological potential of African *Croton* species (Aldhaher et al., 2017; Isyaka et al., 2020; Langat et al., 2008, 2018, 2011, 2012, 2016, 2020a, 2020b; Mulholland et al., 2010; Munissi et al., 2020; Ndunda et al., 2013, 2015, 2016; Terefe et al., 2022a, 2022b, 2023) the chemistry of Kenyan *Croton scheffleri* Pax (Euphorbiaceae) and the investigation into the inhibition of HIV-1 Reverse Transcriptase, the activity against 2 g-positive and 2 g-negative bacterial strains as well as the ability to increase serum starved human dermal fibroblast cell proliferation is reported. *C. scheffleri* is a shrub or small tree, that grows up to 12 m in height, predominantly in the seasonally dry tropical biome, restricted to Kenya, Malawi, and Zambia (Ngumbau et al., 2020). *Croton* is a large genus, with approximately 1300 species, in East Africa there are about 32 species, and *C. scheffleri* is one of the 18 species that occur in Kenya. A decoction of the roots of *C. scheffleri* is used in northern Kenya to treat malaria and fever (Fern, 2021). In Kenya, other *Croton* species are also used in traditional medicinal systems, in some cases this includes bacterial infections and wound healing. For instance, *C. dichogamus*, is used for chest pain, respiratory difficulties and bacterial infections such as gonorrhea (Matara et al., 2021). *C. sylvaticus* is used for boils and swellings (Moremi et al., 2021; Lovett, 1993), and the sap of the young leaves is used to relieve ear infections (Moremi et al., 2021). Kenyan *Croton* species have been reported to predominantly yield diterpenoids, including *ent*-clerodanes (Guetchueng et al., 2018; Langat et al., 2008; Munissi et al., 2020; Ndunda et al., 2016; Terefe et al., 2022a), crotofolanes (Aldhaher et al., 2017; Kawakami et al., 2016; Terefe et al., 2022a), cembranes (Mulholland et al., 2010; Xu et al., 2018), abietanes (Isyaka et al., 2020; Langat et al., 2020b; Ndunda et al., 2016; Sadgrove et al., 2019; Yang et al., 2011), trachylobanes (Munissi et al., 2020), kaurenes (Xu et al., 2018), tiglianes (Xu et al., 2018), and pimarenes (Isyaka et al., 2020; Rayanil et al., 2013; Xu et al., 2018).

In westernised societies, increasing life expectancy and obesity rates have resulted in an increasingly elderly population and higher rates of diabetes (Moses et al., 2023). These morbidities have in turn led to an increasing incidence of non-healing wounds such as diabetic ulcers, venous stasis ulcers and pressure ulcers (Moses et al., 2023). These

* Corresponding author.
E-mail address: s.schwikkard@kingston.ac.uk (S. Schwikkard).

https://doi.org/10.1016/j.phytochem.2025.114460
Received 11 October 2024; Received in revised form 24 February 2025; Accepted 27 February 2025
Available online 28 February 2025

chronic wounds affect the mobility and quality of life of patients and impose significant economic costs on the healthcare systems responsible for treating them (Moses et al., 2023).

The plant family Euphorbiaceae is of particular interest to pharmacognosists and ethnopharmacologists investigating natural products that have the potential to enhance wound healing. For example, in Papua New Guinea, ethnobotanical research indicates plants from the Euphorbiaceae family are often used as treatments for tropical ulcers and skin sores (Prescott et al., 2012). Furthermore, the Australian plant *Fontainea picrosperma* C.T.White (Euphorbiaecae) is the source of the compound tigilanol tiglate (Moses et al., 2020a,b) which is currently in development as a treatment for wound healing *in vivo* and believed to exert its effects by acting on fibroblasts and keratinocytes (Reddell et al., 2021). The Euphorbiaceae family is also renowned as the source of phorbol esters such as the compound ingenol mebutate which has been used as a treatment for early-stage skin cancer (Lebwohl et al., 2012). Phorbol esters are known to act on protein kinase C and therefore are able to regulate cell proliferation.

Considering the association of Euphorbiaceae plants with dermatology and wound healing applications, a logical starting point in the investigation of novel compounds from this family is to assay them for their ability to stimulate dermal fibroblast proliferation. In addition, an investigation into the inhibition of HIV-1 Reverse Transcriptase, proliferation of serum starved dermal fibroblast cells at a concentration of 100 nM and antibacterial activity against *Staphylococcus aureus* 29213 and *Enterococcus faecalis* 29212, as well as gram-negative bacteria *Escherichia coli* 25922 and *Pseudomonas aeruginosa* 27853 was carried out.

2. Results and discussion

The dichloromethane (DCM) and methanol (MeOH) extracts of the stem bark of *C. scheffleri,* and the DCM extract of the leaves of *C. scheffleri* were initially separated by flash column chromatography using silica gel (Merck 9385). Further purification was carried out using silica gel (Merck 7730, mesh 70–230) or Sephadex LH20. Some separations were achieved by preparative thin layer chromatography (PTLC). The stem bark extract of *C. scheffleri* yielded nine undescribed compounds (**1**–**4**, **6**, **7**, **9**, **11** and **12**), and four previously described compounds (**5**, **8**, **10** and **13**), whereas the leaf extracts of *C. scheffleri* provided six known compounds (**14**–**19**), (Fig. 1, Details of compound isolation and spectroscopic Data in Supporting Information, S1, S2). The structures were characterised by their spectroscopic data, including NMR, HRESIMS, IR, UV, optical rotation and ECD (supporting information, S2). The known compounds crotodictyo C **(5)** (Munissi et al., 2020), ermiasolide C **(8)** (Terefe et al., 2022b), ermiasolide B **(10)** (Terefe et al., 2022b), and the indole alkaloid **(13)** (Aderogba et al., 2013) were isolated from *C. megalocarpus* and were identified by comparing the NMR data, HRESIMS, IR and ECD to the reported literature. Ayanin (**14**) (Yuan et al., 2017), pheophytin a (**15**) (Kurihara et al., 2014), ferulic acid (**16**) (Jayaprakasam et al., 2006), 1,3,4-trihydroxybenzene (**17**) (Li et al., 2023), sitosterol (**18**) (Lizazman et al., 2023), and podosterol (**19**) (Liu et al., 2017) compared well to the reported literature. All NMR data for previously undescribed compounds can be found in Tables 1 and 2.

2.1. Characterisation of previously undescribed compounds

Crotoschefflerolide A (**1**) was isolated from the MeOH extract of the bark of *C. scheffleri* as a yellow gum. The molecular formula was determined by HRESIMS as $C_{20}H_{22}O_7$ with the $[M+H]^+$ peak at *m/z* 375.1433, (calcd 375.1444for $[M+H]^+$). NMR data can be found in Tables 1 and 2. The IR spectrum showed absorption bands at 3459 cm^{-1} for O–H stretching, 3016 cm^{-1} and 2958 cm^{-1} for C–H stretches, 1771 cm^{-1} for the lactone carbonyl stretch and 1679 cm^{-1} for a C=C bond stretch. The NMR data indicated a clerodane diterpene with a furan ring at C-12. Characteristic furan carbon peaks could be seen at δ_C 147.7 (C-16, H-16 at δ_H 8.10), δ_C 144.6 (C-15, H-15 at δ_H 7.42), δ_C 108.5 (C-14, H-14 at δ_H 6.71) and δ_C 127.4 (C-13). In addition, the ^{13}C NMR spectrum showed a ketone at δ_C 191.9 (C-12) and two lactone carbonyl groups at δ_C 177.1 (C-20) and δ_C 176.3 (C-19). The presence of four methylene groups at 37.1 (C-11), 28.8 (C-6), 23.7 (C-2) and 20.0 (C-1), four methine groups at 81.6 (C-7), 37.9 (C-10), 46.5 (C-8) and 81.5 (C-3),

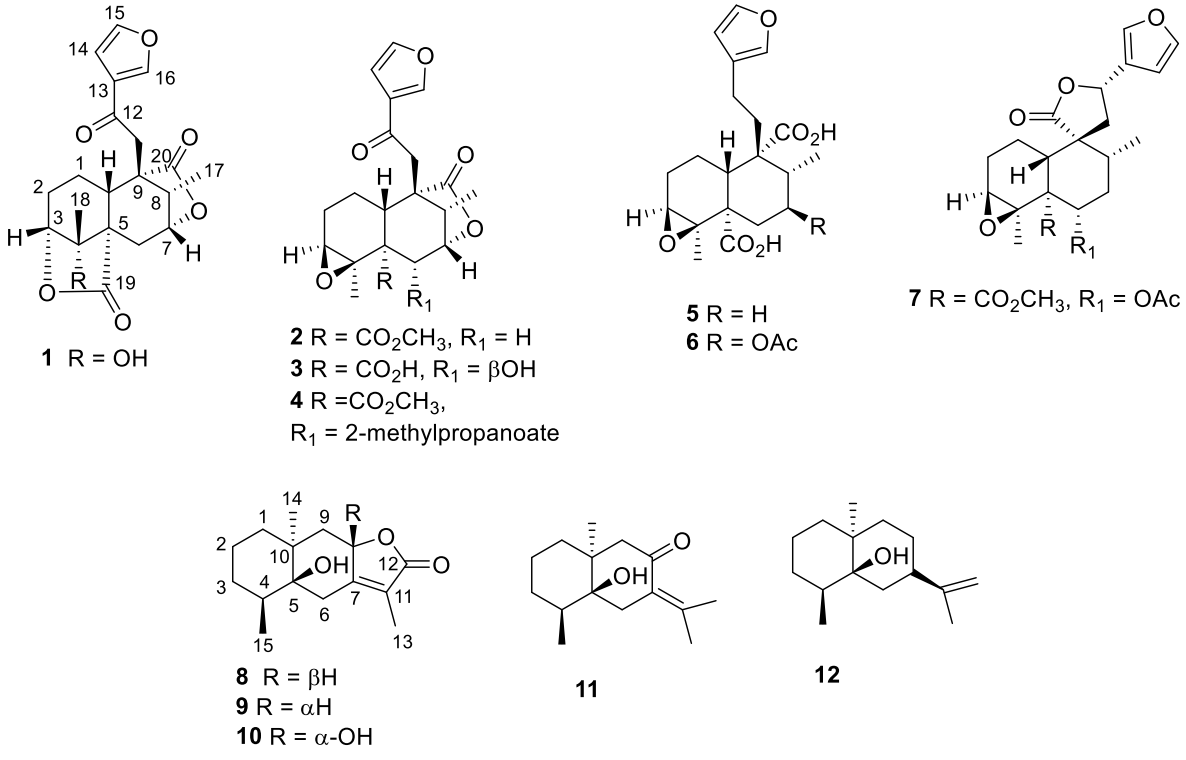

Fig. 1. Clerodane diterpenoids and sesquiterpene lactones isolated from the bark of Kenyan *C. scheffleri.*

Table 1
^{1}H NMR (400 MHz, $CDCl_3$) data for compounds 1–4, 6,7, 9 11 and 12 (*J* in Hz).

position	1	2	3	4	6	7	9	11	12
1	1.38 m	1.07 d (11.1)	1.72 m	1.96 dd (13.7, 4.7)	2.37 m	2.58 dd (4.6, 12.6)	1.90 m	1.52 m	1.62 d (5.4)
	1.78 m	2.28 m	2.10 d (12.4)	1.11 dd (13.7, 6.4)	2.13 m	1.64 dd (12.9, 4.6)	1.62 m	1.52 m	1.33 m
2	1.93 d (4.0)	2.09 d (14.4)	1.25 (s)	2.07 m	2.24 m	2.31 m	1.47 m	1.61 m	1.67 m
	1.78 dd (14.4, 1.4)	1.67 m	1.25 (s)	1.71 m	1.76 m	1.83 m	1.34 m	1.15 m	1.48 m
3	4.10 d (4.0)	2.93 dd (2.3, 14.4)	2.99 (s)	2.93 d (6.4)	3.05 brs ($W_{1/2}$ = 4.7)	2.93 brs ($W_{1/2}$ = 4.0)	1.61 m	1.46 m	1.41 m
	–	–	–	–	–	–	1.17 s	1.35 m	1.41 m
4	–	–	–	–	–	–	1.88 m	2.08 m	1.73 m
5	–	–	–	–	–	–	–	–	–
6	2.22 brs ($W_{1/2}$ = 8.9)	3.10 dd (4.9, 12.5)	4.05 d (9.3)	5.21 d (0.8)	2.29 m	4.92 dd (11.8, 3.8)	2.80 d (14.5)	2.27 d (16.4)	1.73 m, 1.09 m
	1.76 dd (14.4, 2.9)	1.90 d (12.5)	–	–	1.32 m	–	2.30 dd (3.1, 14.5)	2.33 m	–
7	4.50 d (2.9)	4.38 d (4.9)	4.40 brs ($W_{1/2}$ = 2.8 Hz/ppm)	4.18 brs ($W_{1/2}$ = 1.9 Hz/ppm)	5.12 dd (11.2, 2.0)	2.48 m	–	–	2.40 m
	–	–	–	–	–	1.65 m	–	–	–
8	2.61 d (m)	2.67 m	2.72 m	2.84 m	2.09 dd (6.7, 2.0)	1.74 m	4.93 m	–	1.53 m
	–	–	–	–	–	–			1.53 m
9	–	–	–	–	–	–	1.63 m	2.69 dd (1.0, 16.3)	1.59 d (4.4)
		–	–	–			1.50 m	1.97 d (16.3)	1.02 m
10	3.26 d (18.1)	2.28 m	2.19 m	2.48 d (4.7)	1.53 m	1.40 dd (12.6, 1.9)	–	–	–
11	3.36 d (19.2)	2.80 dd (19.3, 2.3)	3.41 d (19.3)	3.50 d (19.5)	1.62 m	2.37 m	–	–	–
	2.71 d (19.2)	3.47 d (19.3)	2.87 d (19.3)	2.93 d (19.5)	1.28 m	2.29 m	–	–	–
12	–	–	–	–	2.42 m	5.39 dd (9.4, 9.7)	–	2.08 s	4.72 d (7.9)
	–	–	–	–	1.89 m	–	–	–	4.72 d (7.9)
13	–	–	–	–	–	–	1.82 s	1.80 s	1.73 s
14	6.71 dd (1.8, 0.8)	6.75 dd (1.8, 0.7)	6.77 d (1.0)	6.77 dd (2.7, 1.0)	6.27 dd (1.8, 0.9)	6.36 dd (0.7, 1.8)	1.17 s	1.05 brs ($W_{1/2}$ = 2.4)	1.02 s
15	7.42 d (1.4)	7.45 t (1.7)	7.48 t (1.6)	7.47 dd (3.3, 0.3)	7.26 brs ($W_{1/2}$ = 0.5)	7.44 brs ($W_{1/2}$ = 2.8)	0.92 d (6.6)	0.94 d (6.7)	0.79 d (6.6)
16	8.10 d (0.8)	8.13 brs ($W_{1/2}$ = 3.1)	8.14 brs ($W_{1/2}$ = 3.2 Hz/ppm)	8.14 d (0.5)	7.38 dd (3.4, 1.6)	7.41 dd (1.7, 1.6)	–	–	
17	0.94 d (6.9)	0.93 d (6.9)	0.96 d (6.9)	0.97 d (6.9)	0.99 d (6.7)	0.99 d (6.4)	–	–	
18	1.22 s	1.43 brs ($W_{1/2}$ = 1.8)	–	1.41 (s)	1.48 s	1.32 s	–	–	
19	–	–	–	–	–	–	–	–	
20	–	–	–	–	–	–	–	–	
19-OCH_3	–				–		–	–	
21-OCH_3				3.81 (s)		3.71 s			
22 (C═O, Ac)	–				–	–	–	–	
22 (CH_3, Ac)	–				2.10 s	–	–	–	
23 (CH_3, Ac)						2.13 s			
OH	–				–	–	3.83 s	3.85 s	3.53 s
1′	–			–	–	–	–	–	
2′	–			2.47 m	–	–	–	–	
3′	–			1.24 d (7.0)	–	–	–	–	
4′	–			1.82 m	–	–	–	–	
	–			1.54 m	–	–	–	–	
5′	–			0.95 m	–	–	–	–	

three quaternary carbon atoms 75.7 (C-4), 52.2 (C-5) and 49.3 (C-9) and two methyl groups 14.6 (C-17) and 22.4 (C-18) were observed. The ^{1}H NMR spectrum displayed a singlet at δ_H 4.78 integrating to 1H assigned to a hydroxy group (OH) at C-4. This peak showed no cross peak in the HSQC and correlated in the HMBC spectrum with C-3 (δ_C 81.5). Two protons at δ_H 4.50 (H-7) and δ_H 4.10 (H-3) correlated with HSQC with carbon peaks at δ_C 81.6 (C-7) and δ_C 81.5 (C-3). HMBC correlations between C-7 (δ_C 81.6) and H-17 (δ_H 0.94) and between C-3 (δ_C 81.5) and H-18 (δ_H 1.22) confirmed their assignments. COSY correlations could be seen between H-7 and H-6α and H-6β as well as between H-3 and H-1. HMBC correlations could be seen between the ketone at C-12 (δ_c 191.9) and H-11α (δ_H 3.36) and H-11β (δ_H 2.71); the lactone at C-20 (δ_c 177.1) and H-8 (δ_H 2.61) and H-10 (δ_H 3.26); the lactone at C-19 (δ_c 176.3) to H-10 (δ_H 3.26) and H-6β (δ_H 1.76). HMBC correlations could also be seen between the C-16 (δ_c 147.7) and H-15 (δ_H 7.42), between C-15 (δ_c 144.6) and C-16 (δ_C147.7) and H-14 (δ_H 6.71), and between the fully substituted C-13 (δ_c 127.4) and C-14 (δ_c 108.5), with H-16 (δ_H 8.10) and H-15 (δ_H 7.42). The COSY spectrum showed coupling between the methyl group proton doublet H_3-17(δ_H 0.94, J = 6.9 Hz) with H-8 (δ_H 2.61). Coupling could also be seen between H-16 (δ_H 8.10) and H-15 (δ_H

Table 2
^{13}C NMR (400 MHz, CDCl3) data for compounds 1–4, 6, 7, 9,11, and 12.

position	1	2	3	4	6	7	9	11	12
1	20.0 CH_2	17.0 CH_2	26.2 CH_2	16.9 CH_2	17.3 CH_2	17.6 CH_2	42.0 CH_2	21.1 CH_2	35.2 CH_2
2	23.7 CH_2	26.8 CH_2	29.7 CH_2	27.0 CH_2	25.4 CH_2	27.4 CH_2	30.2 CH_2	35.2 CH_2	20.8 CH_2
3	81.5 CH	61.7 CH	62.7 CH	62.6 CH	62.3 CH	61.5 CH	34.4 CH_2	30.6 CH_2	30.5 CH_2
4	75.7 C	61.9 C	51.8 C	53.6 C	59.4 C	60.8 C	34.8 CH	23.9 CH	34.5 CH
5	52.2 C	51.1 C	52.5 C	50.1 C	52.5 C	50.4 C	76.8 C	74.2 C	75.1 C
6	28.8 CH_2	37.8 CH	76.0 CH	74.5 CH	36.6 CH_2	74.6 CH	33.6 CH_2	38.2 CH_2	35.8 CH_2
7	81.6 CH	81.4 CH	88.7 CH	84.8 CH	71.6 CH	34.4 CH_2	160.4 C	128.9 C	40.3 CH
8	46.5 CH	49.4 CH	46.6 CH	47.2 CH	34.1 CH	38.8 CH	78.4 CH	203.2 C	26.2 CH_2
9	49.3 C	48.7 C	50.2 C	50.3 C	49.3 C	52.2 C	20.2 CH_2	52.6 CH_2	34.8 CH_2
10	37.9 CH	47.9 CH	44.5 CH	47.1 CH	42.6 CH	52.5 CH	39.2 C	39.3 C	37.1 C
11	37.1 CH_2	37.9 CH_2	37.6 CH_2	37.9 CH_2	17.7 CH_2	41.6 CH_2	123.4 C	147.2 C	150.9 C
12	191.9 C	192.6 C	192.2 C	192.2 C	29.9 CH_2	71.6 CH	175.0 C	23.1 CH_3	108.6 CH_2
13	127.4 C	127.4 C	127.4 C	127.4 C	123.4 C	125.4 C	8.5 CH_3	35.1 CH_3	21.1 CH_3
14	108.5 CH	108.6 CH	108.3 CH	108.6 CH	110.8 CH	108.2 CH	20.8 CH_3	22.3 CH_3	20.6 CH_3
15	144.6 CH	144.7 CH	144.6 CH	144.8 CH	138.9 CH	139.8 CH	15.3 CH_3	15.2 CH_3	15.1 CH_3
16	147.7 CH	147.8 CH	147.6 CH	147.8 CH	143.6 CH	144.3 CH	–	–	–
17	14.6 CH_3	14.9 CH_3	14.4 CH_3	14.3 CH_3	16.2 CH_3	16.3 CH_3	–	–	–
18	22.4 CH_3	20.6 CH_3	22.1 CH_3	21.2 CH_3	23.0 CH_3	23.0 CH_3	–	–	–
19	176.3 C	171.2 C	171.2 C	169.3 C	168.4 C	168.6 C	–	–	–
20	177.1 C	177.8 C	177.7 C	177.4 C	163.4 C	175.2 C	–	–	–
21		50.9 CH_3		51.8 CH_3		–			
19-OCH_3	–	–	–	–	–	–	–	–	–
21-OCH_3	–	–	–	–	–	51.2 CH_3			
21 (C═O, Ac)	–	–	–	–	170.3 C	–	–	–	–
22 (C═O, Ac)	–	–	–	–	–	171.3 C			
22 (CH_3, Ac)	–	–	–	–	21.7 CH_3		–	–	–
23 (CH_3, Ac)	–	–	–	–	–	22.1 CH_3			
1′	–			175.9 C	–	–	–	–	–
2′	–			41.9 CH	–	–	–	–	–
3′	–			16.4 CH_3	–	–	–	–	–
4′	–			26.5 CH_2	–	–	–	–	–
5′	–			11.9 CH_3	–	–	–	–	–

7.42), and H-14 (δ_H 6.71) and H-15 (δ_H 7.42). The relative configuration of compound **1** was determined using the nuclear Overhauser effect (NOESY) spectroscopy. NOESY correlations could be seen between the OH group at C-4 and H-6α as well as between H_3-18 and 6β and 2β. There was no correlation found between H_3-18 and H_3-17. This would suggest that the OH group at C-4 is on the same face of the molecule as H-6α and that H_3-18 and H_3-17 are on opposite sides of the molecule. H-3 also gave a correlation with H_3-18, indicating that they are in proximity (Fig. 4). The absolute configuration was subsequently determined by ECD (Fig. 2) and established compound **1** as an *ent*-clerodane.

Crotoscheffleriolide B (**2**) was isolated as a colourless oil from the MeOH extract of the stem bark of *C. scheffleri*. HRESIMS gave a peak at *m/z* 389.1594 (calcd 389.1556 $[M]^+$), indicating a molecular formula of $C_{21}H_{24}O_7$ and ten degrees of unsaturation. The FTIR spectrum showed absorption bands at 3135 cm^{-1} and 2955 cm^{-1} for C–H stretches, at 1777 cm^{-1} indicating the presence of a carbonyl methyl ester stretch, at 1742 cm^{-1} for the C═O stretch of an aliphatic ester, 1721 cm^{-1} for a C═O stretch of an aliphatic ketone, at 1672 cm^{-1} for the C═C stretch, and 1158 cm^{-1} for the C–O ester stretch. The ^{1}H NMR spectrum revealed the presence of a furan ring with resonances at δ_H 6.75 (dd, J = 1.7, 0.8 Hz), δ_H 7.45 (d, J = 1.7 Hz), and δ_H 8.13 (brs, $W_{1/2}$ = 3.1 Hz), for H-14, H-15, and H-16 respectively; and two methyl group proton resonances at δ_H 1.43 (brs, $W_{1/2}$ = 1.8 Hz) and δ_H 0.93 (d, J = 6.9 Hz), for H_3-18, and H_3-17 respectively. The ^{13}C and DeptQ NMR spectra showed 21 carbon resonances, including one methoxy group, two methyl groups, four methylene groups, seven methine groups, and seven fully substituted carbon resonances. A carbon resonance at δ_c192.6 (C-12) indicated the presence of a ketone carbonyl group, while δ_c 177.8 (C-20) and δ_c 171.2 (C-19) revealed the presence of a lactone group and a methyl ester. The four carbon resonances typical of a furan ring were present at δ_c 147.8 (C-16), δ_c 144.7 (C-15), δ_c 127.4 (C-13), and δ_c 108.6 (C-14). The resonance at δ_c 81.4, typical of a carbon directly bonded to an oxygen atom was assigned to C-7 and the two carbon resonances at δ_c 61.9 (C-4) and 61.3 (C-3) showed the presence of an epoxy group at between C-3 and C-4.

The HMBC NMR spectrum showed correlations between the ketone carbon resonance at δ_c 192.6 (C-12) and the two methylene proton resonances at δ_H 2.80 (dd, J = 19.3, 2.3 Hz, H-11α), and δ_H 3.47 (d, J = 19.3 Hz, H–11β). The corresponding carbon resonance for H_2–11 was assigned using the HSQC/DEPTQ spectrum as occurring at δ_c 37.9. Correlation between the lactone carbon resonance at δ_c 177.8 (C-20) and the proton resonances at δ_H 4.38 (d, J = 4.9 Hz, H-7), δ_H 2.80 (dd, J = 19.3, 2.30 Hz, H–11α) and δ_H 2.67 (m, H-8) where observed in the HMBC. The HSQC/DEPTQ spectrum assigned the corresponding carbon resonances for H-7 and H-8 at δ_c 81.4 and δ_c 49.4, respectively. The HMBC correlations between the methyl ester carbonyl group at δ_c 171.2 (C-19) and the methine proton resonance at δ_H 2.28 (H-10, m), the methylene resonance at δ_H 2.28 (H-1β, m) and the methylene resonance at δ_H 1.90(d, J = 12.5 Hz, H-6β) were likewise observed. The corresponding carbon resonances for H-10, H_2-1, and H_2-2 were assigned using the HSQC/DEPTQ spectrum, as δ_c 47.9, δ_c 17.0 and δ_c 26.8, respectively. The epoxy group carbon resonances at δ_c 61.9 (C-4) and δ_c 61.7 (C-3) showed a correlation in the HMBC spectrum with the methyl resonance at δ_H 1.43 (brs, $W_{1/2}$ = 1.80 Hz/ppm, H_3-18), the resonance at δ_H 2.09 (d, J = 14.4 Hz, H-2α), and the resonance at δ_H 1.07 (d, J = 11.1 Hz, H-1α). The corresponding carbon resonances for H_3-18, H_2-2, and H_2-1 were determined by HSQC to be δ_c 20.6, δ_c 26.8, and δ_c 17.0, respectively. C-18 (δ_c 20.6) was correlated in the HMBC spectrum to the multiplet at δ_H 1.67 (H-2β) and to δ_H 1.07 (d, J = 11.1 Hz, 2H-1α). The corresponding carbon resonances for H_2-2 and H_2-1 have been observed in the HSQC/DETQ spectrum as δ_c 26.8 and δ_c 17.0, respectively. The methyl group at δ_H 0.93 (d, J = 6.9 Hz, 3H-17) was correlated in the HMBC spectrum to C-7 (δ_c 81.4) and C-8 (δ_c 49.4). Coupling between the furan proton peaks was seen in the COSY spectrum. The methine proton at δ_H 2.67 (m, H-8) is coupled to the methyl group proton resonance at δ_H 0.93 (H_3-17). While the methylene protons at δ_H 2.80 (dd, J = 19.3, 2.30 Hz, H-11α) and δ_H 3.47 (d, J = 19.3 Hz, H-11β) are coupled to each other. Coupling in the COSY can also be seen between δ_H 3.10 (dd, J =

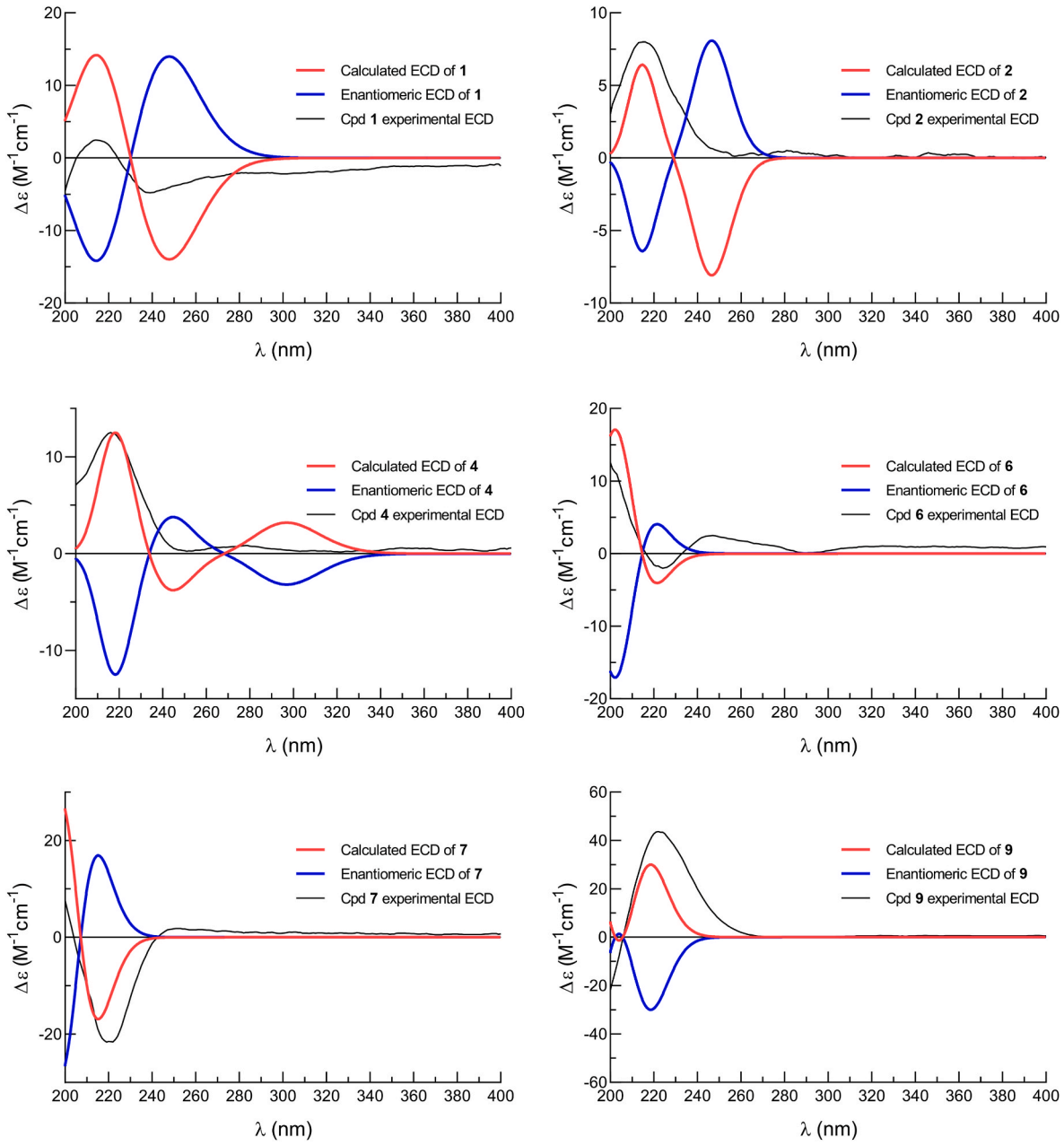

Fig. 2. ECD spectrum for compounds **1, 2, 4, 6, 7,** and **9.**

4.9, 12.5 Hz, H-6α) and δ_H 4.35 (d, J = 4.9 Hz, H-7), the methylene proton at δ_H 2.09 (d, J = 14.4 Hz, H-2α) and δ_H 1.67 (m, H-2β), and between δ_H 1.07 (d, J = 11.1 Hz, H-1α). Relative stereochemistry was established using NOESY spectroscopy with correlations noted between H-11α and the methoxy group of the methyl ester at C-19, as well as H_3-17, indicating that they are all on the same face of the molecule. H-7 correlates with H-6β and H-10 with H-2β, indicating that they are on the same face of the molecule. NOESY correlations could also be seen between H_3-18 and H-3 as well as H-6α, indicating that they were on the same side of the molecule (Fig. 4). The absolute configuration was determined by ECD and the experimental curve matched the calculated trace for the *ent*-clerodane skeleton (Fig. 2).

Crotoscheffleriolides C (**3**) and D (**4**) both share the same basic skeleton as crotoscheffleriolide B (**2**). Both are clerodane diterpenoids with a ketone at C-12 (δ_c 192.2 for both compounds), a lactone at C-20 (δ_c177.7 and δ_c 177.4 respectively), a furan at C-12 and an epoxide between C-3 and C-4 (δ_c 62.7 and 51.8 for crotoscheffleriolide C and δ_c 62.6 and 53.6 for crotoscheffleriolide D). Crotoscheffleriolide C (**3**) differed from Crotoscheffleriolide B (**2**) in that a hydroxy group was present at C-6 (δ_c 76.0, δ_H 4.05, d, J = 9.3) and a carboxylic acid group at C-19 (δ_c 171.2). HSQC correlations could be seen between H-6 and a peak at δ_c 76.0 (C-6). A peak at δ_H 3.74, with no correlation in the HSQC, was assigned to the OH group at C-6. An HMBC correlation could be seen between this OH group and C-7 (δ_c 88.7). NOESY spectroscopy confirmed that H_3-18, H-3 and H-6 were all on the same face of the molecule in addition to a correlation being noted between H-7 and H-8, indicating that they were likewise on the same face of the molecule. The formula for Crotoscheffleriolides C (**3**) has a molecular formula of$C_{20}H_{22}O_8$ as determined by NMR. The HREIMS gave m/z 389.1594 (calcd $[M\text{-}H]^+$ m/z 389.1236). This lies outside the 5 ppm difference required for HRMS, but the NMR data remains convincing. Crotoscheffleriolides D (**4**) contained a methyl ester at C-19 (δ_c 169.3) and a 2-methylpropanoate group at C-6 (δ_c 74.5). A methoxy methyl group proton resonance was clear at δ_H 3.81, and this correlated in the HSQC to

the carbon resonance at δ_c 51.8. An HMBC correlation could be seen between the methoxy methyl group proton resonance (δ_H 3.81) and C-19 (δ_c 169.3). Additional HMBC correlation could be seen between C-19 and H-6 (δ_H 5.21, d, $J = 0.80$ Hz). The carbonyl group of the 2-methyl-propanoate group correlated in the HMBC spectrum with H-6 (δ_H 5.21) and H-21, the methoxy methyl group proton resonance (δ_H 3.81), confirming its position at C-6. In addition, COSY correlations could be seen between H-2' (δ_H 2.47, m) and H-3' (δ_H 1.24, d, $J = 7.04$ Hz) as well as between H-2′ and H-4' (δ_H 1.54 m) and between H-5' (δ_H 0.95 m) and H-4α' (δ_H 1.82 m) and H-4′β (see Fig. 3). NOESY correlations were noted between H-11α and the methyl ester methyl group as well as between H-6 and H-8, H_3-18 and H_3-17 and H_3-18 and H-3. This would suggest the same relative stereochemistry as crotoscheffleriolide C (**3**). The molecular formula for Crotoscheffleriolide D (**4**) of $C_{26}H_{32}O_9$ was confirmed by HREIMS with $[M+H]^+$ m/z 489.2119 (calcd 489.2125for $[M+H]^+$). Absolute configuration for crotoscheffleriolide D (**4**) was confirmed by ECD (Fig. 2). Due to small amounts, the ECD was not recorded for crotoscheffleriolide C (**3**), but it was determined to be an *ent*-clerodane based on similarity of relative stereochemistry to crotoscheffleriolides D (**4**).

Crotoscheffleriolide E (**6**) had the same basic clerodane skeleton as Crotodictyo C **(5)** (Munissi et al., 2020), isolated from *Croton dictyophlebodes*, with the addition of an acetate group at C-7. HREIMS confirmed a molecular formula of $C_{22}H_{28}O_8$ with an $[M+H]^+$ peak at *m/z* 421.1855 (421.1862 calcd for $[M+H]^+$). As seen with compounds **2**, **3**, **4** and **5**, compound **6** had an epoxide at carbon 3 and 4 (δ_C 62.3 and 59.4 respectively), a furan at C-12 (C-13 δ_C 123.4, C-14 δ_C 110.8, C-15 δ_C 138.9 and C-16 δ_C143.6) and like compound **3** a carboxylic acid group at C-19 (δ_C 168.4). The absence of the lactone at C-20 was noted due to the absence of the lactone carbonyl peak typically found between δ_C 177.1 and δ_C 177.8. Instead, a carboxylic acid carbonyl peak was seen at δ_C 163.4 (C-20). HMBC correlations between C-20 and H-7 (δ_H 5.12) and C-20 and H-10 (δ_H 1.53) confirmed this assignment. The acetate at C-7 was confirmed by the presence of the acetate carbonyl group carbon resonance (C-21) at δ_C 170.3 and the acetate methyl group carbon peak (C-22) at δ_C 21.7 (δ_H 2.10, s). HMBC correlations were seen between C-21 and H-22 as well as between C-22 (δ_C 21.7) and H-6α (δ_H 2.29). Unlike the previously described compounds, no ketone was noted at C-12 due to the absence of the ketone carbonyl carbon resonance at δ_C192. This was replaced by a methylene resonance at δ_C 29.9 ($\delta_{H\alpha}$ 2.42, $\delta_{H\beta}$ 1.89). HMBC correlations could be seen between C-12 and H_3-17 (δ_H 0.99, d, $J = 6.7$ Hz). NOESY correlations could be seen between H_3-18 and H-3 as well as between H_3-18 and H-7, confirming the relative stereochemistry at C-7 as beta. NOESY correlations were also noted between H-6β and H-1β as well as H_3-17 and H-12α (Fig. 4). Absolute configuration was confirmed by ECD (Fig. 2).

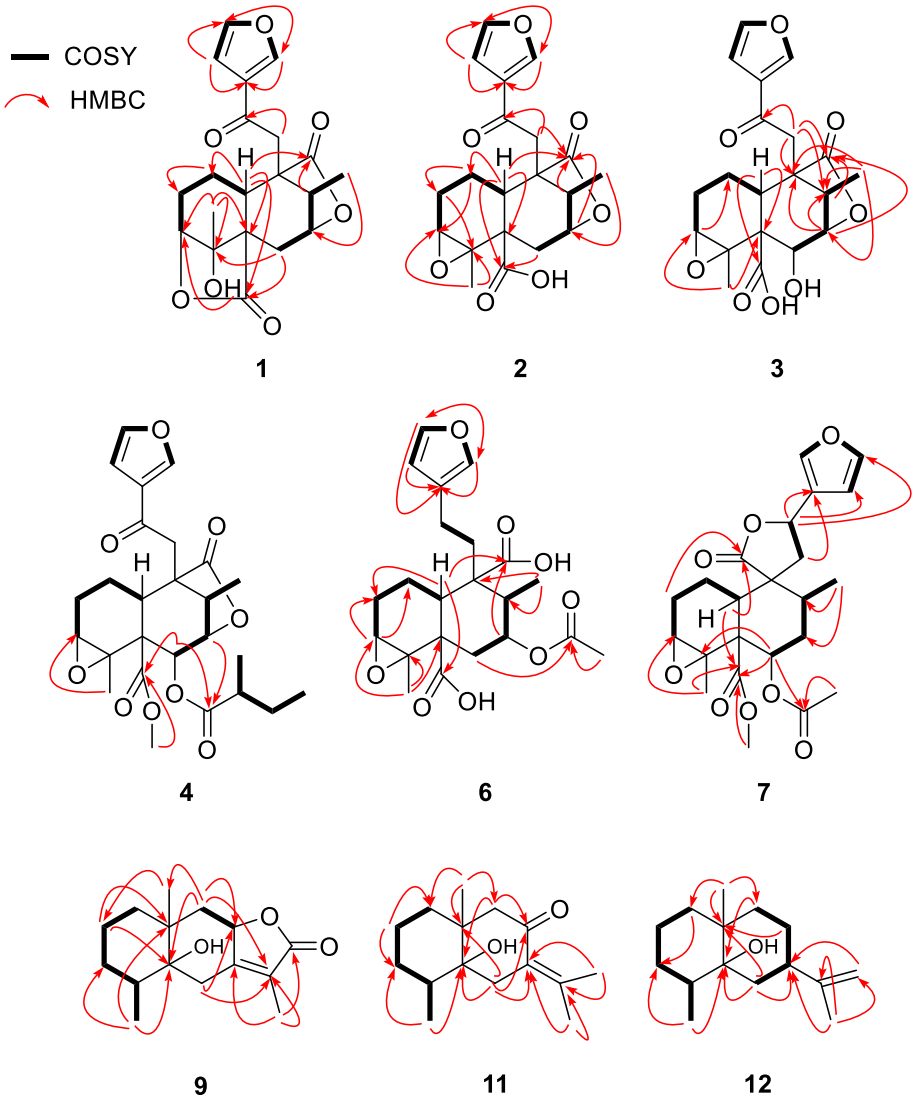

Fig. 3. HMBC and COSY correlations for compounds **1**, **2**, **3**, **4**, **6**, **7**, **9**, **11** and **12**.

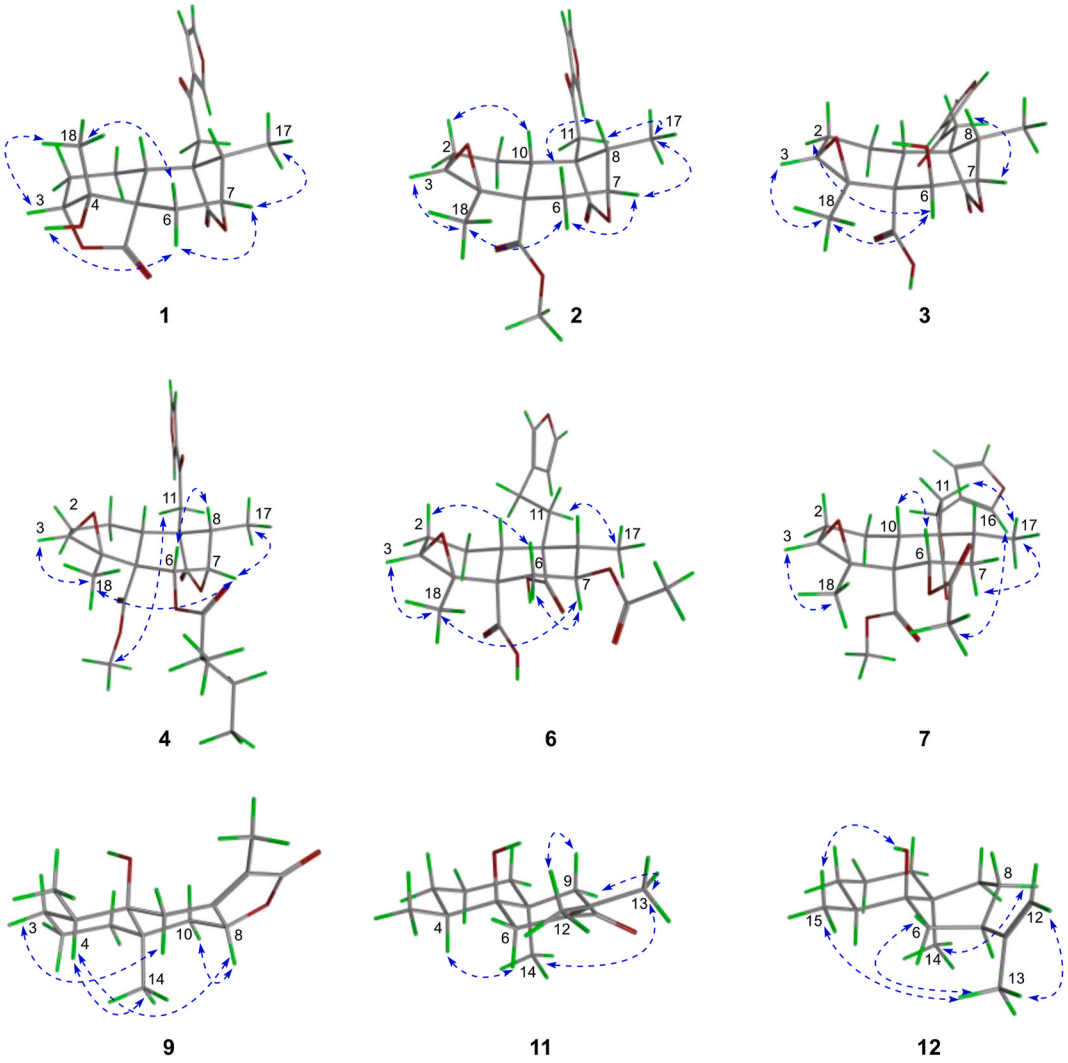

Fig. 4. NOESY correlations for compounds **1, 2, 3, 4, 6, 7, 9, 11** and **12**.

HREIMS indicated a molecular formula of $C_{23}H_{28}O_8$ for Crotoscheffleriolide F (**7**) with $[M+H]^+$ at *m/z* 433.1857 (calcd for $[M+H]^+$ *m/z* 433.1862). Changes in the chemical shifts for the furan carbon and proton resonances (see Tables 1 and 2), together with the presence of a lactone carbonyl resonance at δ_C 175.2, suggested a spirocyclic lactone at C-9. This was confirmed by HMBC correlations between C-20 and H-2α (δ_H 2.31) and H-10 (δ_H 1.40). In addition, H-12 was noted at δ_H 5.39. HMBC correlations between H-12 and C-13 (δ_C 125.4), C-14 (δ_C 108.2) and C-15 (δ_C 139.8) further confirmed the presence of the lactone. As seen previously, an epoxide was present between C-3 and C-4 (δ_C 61.5 and δ_C 60.8 respectively) and a methyl ester at C-19 (δ_C168.6 and δ_C 51.2 for the carbonyl carbon resonance and the methyl ester methyl group carbon resonance respectively). HMBC correlations could be seen between C-19 (δ_C 168.6) and H-6 (δ_H 4.92), the methoxy group (δ_H 3.71) and H-10 (δ_H 1.40). An acetate group was seen at C-6 (δ_C 74.6, δ_H 4.92). The acetate carbonyl carbon resonance (C-22, δ_C 171.3) correlated in the HMBC to the acetate methyl group protons (δ_H 2.13, s) as well as to H-6 (δ_H 4.92). HMBC correlations could be seen between H_3-17 and C-5 (δ_C 50.4), C-8 (δ_C 38.8) and C-7 (δ_C 34.4). NOESY correlations between H-6 and H-8 suggested that they were on the same side of the molecule, with a correlation between H_3-23 (δ_H2.13) and H-14 (δ_H 6.36) suggesting likewise. Correlations were also noted between H_3-18 and H-3 (Fig. 4). Absolute configuration was determined by ECD (Fig. 2).

The sesquiterpene crotoscheffleriune G (**9**) was isolated as a white powder from the MeOH extract of the stem bark *C. scheffleri*. The HRESIMS yielded a $[M+H]^+$ peak at *m/z* 251.1647 (calcd 251.1647), indicating a molecular formula $C_{15}H_{23}O_3$ and five degrees of unsaturation. The FTIR spectrum showed absorption bands at 3490 cm^{-1} for an O–H stretch, at 2931 and 2859 cm^{-1} for -C-H alkyl stretches, at 1736 cm^{-1} for a lactone group, at 1681 cm^{-1} for an alkene stretch and at 1034 cm^{-1} for a C–O stretch.

The ^{13}C and DeptQ NMR spectra showed the presence of fifteen carbon resonances with three methyl groups, five methylene groups, two methine groups and five fully substituted carbon resonances. The three methyl groups proton resonances at δ_H 1.17 (s), δ_H 0.92 (d, $J = 6.6$ Hz), and δ_H 1.82 (s), were assigned to H_3-14, H_3-15, H_3-13 respectively. The full substituted carbon resonance at δ_c 175.0 (C-12) indicated the presence of a lactone group, while the two full substituted carbons resonances at δ_c 123.4 (C-11) and δ_c 160.4 (C-7) were attributed to the olefinic bond. The ^1H NMR spectrum showed the presence of the CO group with a resonance at δ_H 4.93 (m) for H-8 (C-8 at δ_c 78.4) An hydroxy group (OH) resonance at δ_H 3.83 (s), was identified by the lack of a corresponding cross peak in the HSQC spectrum. A fully substituted carbon resonance at δ_c 76.8 was assigned to C-5 and the hydroxy group was placed at C-5 due to HMBC correlations between this hydroxy group resonance (δ_H 3.83) and C-10 (39.2), C-5 (δ_c 76.8) and C-6 (δ_c 33.6). The HMBC spectrum, showed the correlation between the carbon resonance of lactone δ_c 175.0 (C-12) and the methyl group proton resonance δ_H 1.82 (s) (H_3-13), the corresponding carbon resonance for H_3-13 was assigned using the HSQC/DEPTQ spectrum and found to be at δ_c 8.5. The

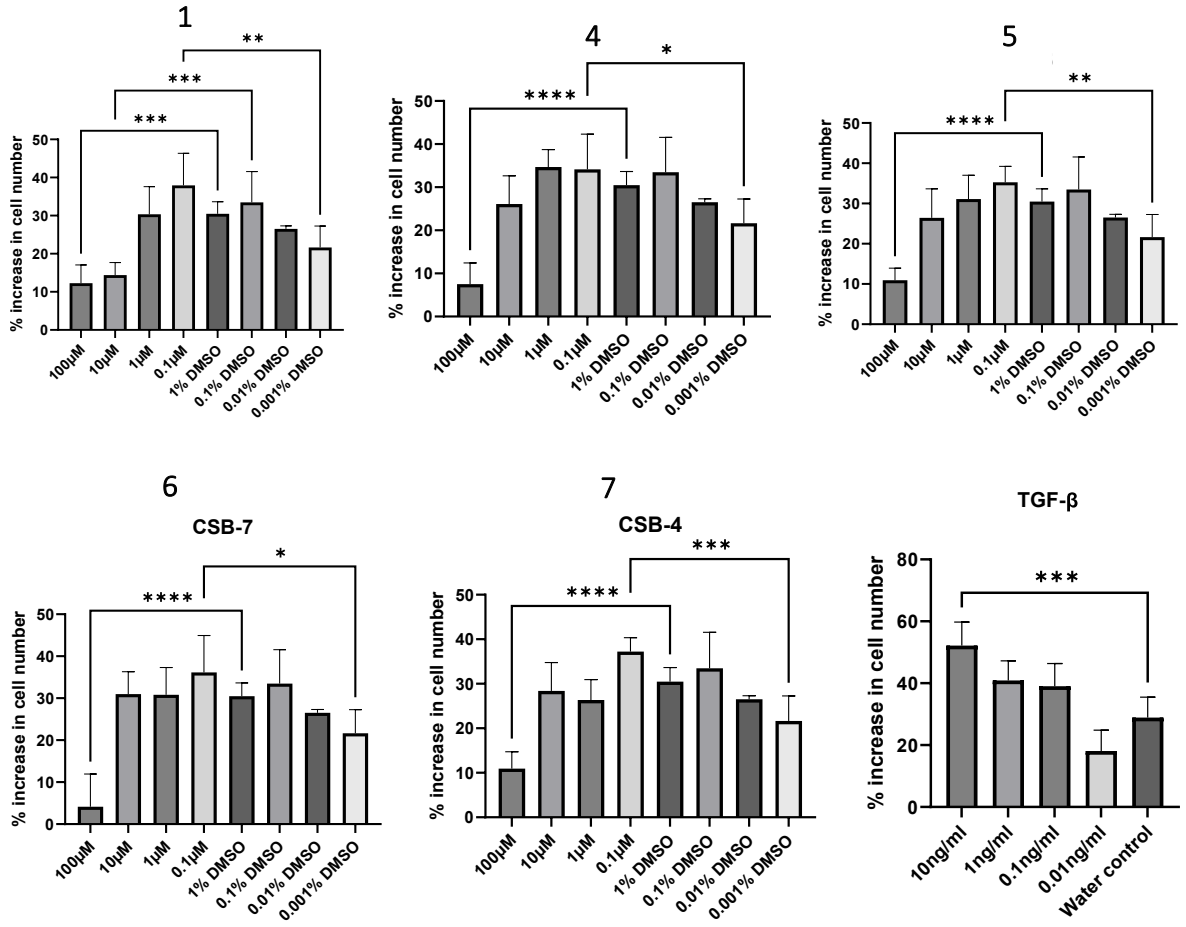

Fig. 5. Effect of compounds crotoscheffleriolide A (**1**), crotoscheffleriolide D (**4**), crotodictyo C (**5**), crotoscheffleriolide E (**6**), crotoscheffleriolide F (**7**) and TGF-β on serum starved normal dermal fibroblasts at 72 h. Error bars indicate standard deviation based on data analysis from n = 4 replicates. DMSO % indicates % v/v of DMSO solvent vehicle controls, comparisons of each compound were made with the corresponding DMSO control. Multiplicity adjusted *p* values: crotoscheffleriolide A (**1**), ***p 0.0006, ***p 0.0004, **p 0.0021. Crotoscheffleriolide D (**4**), ****$p < 0.0001$, *p 0.0191. Crotodictyo C (**5**) ****$p < 0.0001$, **p 0.0048. Crotoscheffleriolide E (**6**), ****$p < 0.0001$, *p 0.0132. Crotoscheffleriolide F (**7**) ****$p < 0.0001$, ***p 0.0006. For TGF-β, changes in cell number were compared to cells treated with a water control.

olefinic carbon resonance at δ_c 123.4 (C-11) was correlated in the HMBC to three protons resonances at δ_H 2.80 (d, J = 14.5 Hz, H-6α), δ_H 2.30 (dd, J = 3.1, 14.5 Hz, H-6β), and δ_H 1.82 (s, H_3-13), the corresponding carbons resonances for H_2-6 and H_3-13was assigned by HSQC/DEPTQ spectrum and occurred at δ_c 33.6 for C-6 and δ_c 8.50 for C-13 respectively. The olefinic carbon resonance at δ_c 160.4 (C-7) was correlated in the HMBC to the proton resonance δ_H 1.82 (s, H_3-13); the methine carbon resonance at δ_c 78.4 (C-8) was correlated to two protons resonances δ_H 2.80 (d, J = 14.5 Hz, H-6α) and δ_H 1.63 (m, H-9α), where the corresponding carbon resonance for H_2-9 was assigned by HSQC/DETPQ as δ_c 20.2. The fully substituted carbon resonance at δ_c 39.2 (C-10) correlated in the HMBC spectrum to four protons resonances at δ_H 1.17 (s, H_3-14), δ_H 1.61 (m, H-3α), δ_H 1.17 (s, H-3β) and δ_H 2.80 (d, J = 14.5 Hz, H-6α); the methylene carbon resonance at δ_c 42.0 (C-1) was correlated to two proton resonances at δ_H 1.17 (s, H_3-14), and δ_H 1.17 (s, H-3β); while the methine carbon resonance at δ_c 34.8 (C-4) was correlated to the methyl group at δ_H 0.92 (d, J = 6.6 Hz, H_3-15). The methylene group at δ_c 33.6 (C-6) was correlated to the methyl group at δ_H 0.92 (d, J = 6.6 Hz, H_3-15); while the methylene group at δ_c 34.4 (C-3) was correlated to two protons resonances at δ_H 1.17 (s, H-3β), and at δ_H 0.92 (d, J = 6 Hz, H_3-15). The methyl group at δ_c 20.8 (C-14) was correlated to three protons resonances at δ_H 0.92 (d, J = 6.6 Hz, H_3-15), δ_H 1.63 (m, H-9α), and δ_H 1.34 (H-2β).

The COSY spectrum showed coupling between the methine group at δ_H 4.93 (m, H-8) and the two protons resonances at δ_H 1.63 (m, Hα-9), and δ_H 2.80 (d, J = 14.5 Hz, H-6α); while the methylene group at δ_H 1.63 (m, H-9α) was coupled to three protons resonances at δ_H 4.93 (m, H-8), δ_H 1.17 (H_3-14), and δ_H 1.90 (m, H-1α). The methine group at δ_H 1.88 (m, H-4) was coupled to the methyl group at δ_H 0.92 (d, J = 6.6 Hz, H_3-15); while the methylene group at δ_H 1.61 (m, H-3α) was coupled to four protons resonances at δ_H 1.17 (s, H-3β), δ_H 1.90 (m, H-1α), δ_H 1.88 (m, H-4), and δ_H 1.34 (m, H-2β). The proton at δ_H 1.47 (m, H-2α) was coupled to δ_H 1.62 (m, H-1β); The relative stereochemistry was confirmed by NOESY spectroscopy. A correlation was seen between H-8 (δ_H 4.93) and H-4α, H-9α and H-3α. A correlation was noted between H_3-14 (δ_H 1.17) and H-4 (δ_H 1.88) and there was no correlation between the hydroxy group at C-5 with any of the above-mentioned proton peaks, confirming the orientation as β (Fig. 4). The absolute configuration was determined by ECD and the experimental trace compared well with the calculated trace for CrotoScheffleriune G (**9**) (Fig. 2).

Ermiasolide C **(8)** and ermiasolide B **(10)** (Terefe et al., 2022b) were both isolated previously from the Kenyan *Croton megalocarpus* and the data compares well with that reported by Terefe et al. (2022b).

Crotoscheffleriune H (**11**) was isolated as an oily pale-yellow substance. The molecular formula was confirmed as $C_{15}H_{24}O_2$, *m/z* 237.1851 $[M+H]^+$ (calculated$[M+H]^+$, *m/z* 237.1854). The FTIR spectrum showed the absorption bands for a hydroxy group stretch at 3475 cm^{-1}, a CH stretch at 2927 and 2856 cm^{-1}, and a ketone carbonyl

group at 1717 cm^{-1}. The ^{13}C NMR spectrum showed fully substituted carbon resonances for a ketone carbonyl group at δ_c 203.2 (C-8), for two olefinic carbon resonances at δ_c 128.9 (C-7) and δ_c 147.2 (C-11) and a carbon with a hydroxy group at δ_c 74.2 (C-5), along with four methyl groups at δ_c35.1 (C-13, δ_H 1.80, s, H_3-13), δ_c23.1 (C-12, δ_H 2.08, s, H_3-12), δ_c 15.2 (C-15, δ_H 0.94 d, $J = 6.7$ Hz, H_3-15) and δ_c 22.3 (C-14, δ_H 1.05 s, H_3-14) and five methylene groups at δ_c38.2 (C-6), δ_c 21.1 (C-1), δ_c35.2 (C-2), δ_c 30.6 (C-3), δ_c 52.6 (C-9). HMBC correlations were clear between C-7 and C-11 and both H_3-13 (δ_H 1.80) and H_3-12 (δ_H 2.08). The position of the carbonyl group at C-8 (δ_c 203.2) was confirmed by the HMBC correlations with H-9α and H-9β, with H-9α also showing correlations with C-11 (δ_c 147.2). H_3-15 correlated with C-3 (δ_c 30.6) and H_3-14 with C-2 (δ_c 35.2), C-5 (δ_c 74.2) and C-10 (δ_c 39.3). NOESY correlation could be seen between H_3-15 (δ_H 0.94) and H_3-13 (δ_H 1.80), as well as between H_3-12 (δ_H 2.08) and H_3-13 (δ_H 1.80) and H-9α (δ_H 2.69) and H-9β (δ_H 1.97) (Fig. 4).

Crotoscheffleriune I (**12**) differed from the compound **11** in that the ketone at C-8 was now a methylene group (C-8, δ_C 26.2, 2H-8 at δ_H 1.53) and the fact that the double bond between C-7 and C-11 in compound **11**, was now between C-11 (δ_C 150.9) and C-12 (δ_C 108.6, H_2-12 at δ_H 4.72, d, $J = 7.9$ Hz). In addition, 3 further methyl groups were present, H_3-14 (δ_C 20.6, δ_H 1.02), H_3-15 (δ_C 15.1, δ_H 0.79, d, $J = 6.6$ Hz)_and H_3-13 (δ_C 21.1, δ_H 1.73). A hydroxy group was found to be present at C-5 (δ_C 75.1). The OH peak was located at δ_C 3.53 (s) as shown by no cross peak in the HSQC when the sample was run in DMSO. Clear HMBC correlations between C-5 (δ_C 75.1) and H_3-14 (δ_H 1.02) and H_3-15 (δ_H 0.79, d, $J = 6.6$ Hz) were observed. In addition, HMBC correlations were seen between H_3-13 (δ_H 1.73) and C-11 (δ_C 150.9) and between H_3-13 (δ_H 1.73) and C-12 (δ_C 108.6). The relative stereochemistry was determined by NOESY spectroscopy. Correlations could be seen between H_3-13 and H_3-15, suggesting that these groups are on the same face of the molecule. A correlation was noted between H_3-15 and the OH group at C-5, suggesting that these were on the same face of the molecule. Limited compound quantities prevented the acquisition of an ECD to establish absolute configuration, but relative stereochemistry established by NOESY spectroscopy would suggest the same absolute configuration as seen in compounds **8**, **9**, **10** and **11**. The base peak obtained by HRMS was noted at m/z 217.1585 $[M-5]^+$, (calcd $[M-5]^+$, m/z 217.1592).

2.2. The effects of the test compounds on serum starved human dermal fibroblast cells

Fibroblasts from chronic wounds are known to exhibit significantly impaired proliferative and migratory responses compared to those derived from healthy skin. This is believed to be a consequence of enhanced cellular senescence within the chronic wound environment (Wall et al., 2008). A hallmark of chronic non-healing wounds is a prolonged inflammatory phase resulting from the activities of neutrophils and M1 macrophages which prevents progression of the wound to a healing phase. The chronic wound environment is characterised by increased protease activity due to the expression of matrix-metalloproteinases (MMPs) and higher level of oxidative stress due to the presence of reactive oxygen species (ROS) (Wall et al., 2008). The high levels of MMPs and ROS has detrimental effects on wound fibroblasts which become senescent and exhibit a slowed growth rate. Fibroblast dysfunction is thought to be connected to irreversible growth arrest or replicative senescence (Wall et al., 2008). Compounds that increase the proliferation of dermal fibroblasts may prove effective as topical treatments for chronic non-healing wounds (Moses et al., 2020a, b). The application of recombinant growth factors to chronic wounds, including fibroblast growth factor, has been proposed as a treatment option, but their susceptibility to proteases in the chronic wound environment has limited their clinical efficacy (Yamakawa and Hayashida, 2019).

The effects of the test compounds on serum starved human dermal fibroblast cells were examined, using live cell cytometry to count cells before addition of test compounds and again at 72 h. Cells treated with the positive control TGF-β exhibited increased cell proliferation as expected. Compounds crotoscheffleriolide D (**4**), crotoscheffleriolide F (**7**), crotodictyo C **(5)**, crotoscheffleriolide A (**1**), crotoscheffleriolide E (**6**), ermiasolide B (**10**), crotoscheffleriune I (**12**) and podosterol (**19**) all induced increased proliferation at 100 nM concentration (Fig. 5, S3). Interestingly, this concentration would be expected to be easily achieved if the plant extract were applied directly to a non-healing ulcer. At higher concentrations many of the compounds acted to inhibit cell proliferation. Indeed, all the compounds inhibited cell proliferation at 100 μM. Furthermore, crotoscheffleriolide A (**1**), crotoscheffleriolide D (**4**) and podosterol (**19**) all inhibited fibroblast proliferation at 10 μM.

Compounds crotoscheffleriolide D (**4**), crotoscheffleriolide F (**7**), crotodictyo C (**5**), crotoscheffleriolide A (**1**), crotoscheffleriolide E (**6**), ermiasolide B (**10**), crotoscheffleriune I (**12**) and podosterol (**19**) should all be investigated further using transcriptomics to help understand the mechanisms of action by which they stimulate fibroblast proliferation.

2.3. Assessment of test compounds for anti-bacterial activity

Initial compound screening for antibacterial activity was performed against four clinical bacterial strains, 2 g-positive, *Enterococcus faecalis* and *Staphylococcus aureus* and 2 g-negatives, *Escherichia coli* and *Pseudomonas aeruginosa*, and growth inhibition determined. Samples (DCM and MeOH extracts of both stem bark and leaves) and pure compounds (**1, 2, 4–13** and **19**) were resuspended in 100% DMSO (VWR) at 200 mg/mL and 10 mg/mL and tested at a final concentration of 1 mg/mL and 50 μg/mL, respectively. Due to limitation of sample amount, pure compounds **3** and **11** were tested only against *S. aureus* and *E. faecalis*.

Compounds and extracts were found to be inactive against the bacterial strains tested. In initial screening assays of extracts from twigs and leaves of *C. scheffleri* sample precipitation was observed when added into aqueous assay medium, thus resulting in falsely higher absorbance measurements at initial time point. Consequently, when bacteria growth inhibitions were calculated, after 24 h of incubation, they were mistakenly overestimated (Figs. 6 and 7). Visual assessments were also taken in parallel, confirming the lack of antibacterial activity of samples.

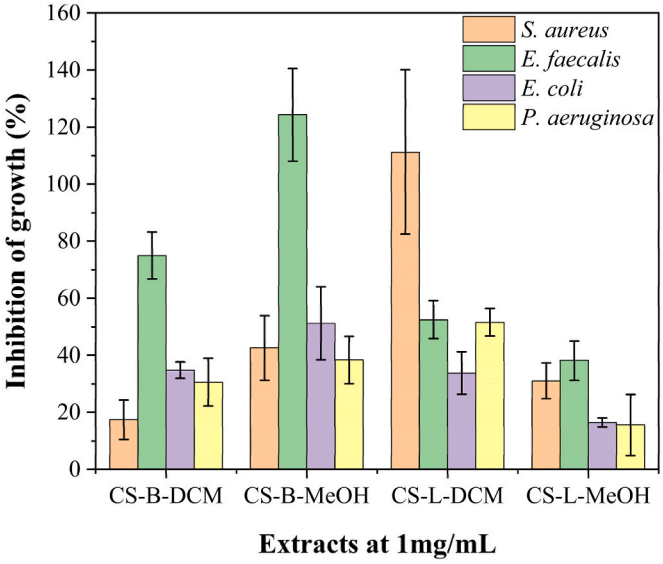

Fig. 6. Screening of extracts *Croton scheffleri* bark DCM and MeOH (CS–B-DCM and CS-B-MeOH) and *Croton scheffleri* leaves DCM and MeOH (CS-L-DCM and CS-L-MeOH) at 1 mg/mL against 2 g-positive (*Staphylococcus aureus* ATCC 29213 and *Enterococcus faecalis* ATCC 29212) and 2 g-negative (*Escherichia coli* ATCC 25922 and *Pseudomonas aeruginosa* ATCC 27853) bacterial strains. Experiments were performed once in triplicate for each strain. Bars indicate average with respective standard deviation.

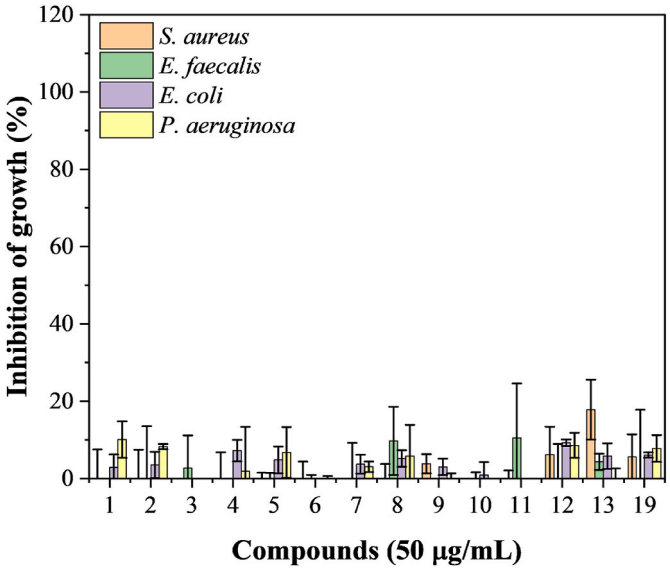

Fig. 7. Screening of compounds **1**–**13** and **19** (50 µg/mL) against 2 g-positive (*Staphylococcus aureus* ATCC 29213 and *Enterococcus faecalis* ATCC 29212) and 2 g-negative (*Escherichia coli* ATCC 25922 and *Pseudomonas aeruginosa* ATCC 27853) bacterial strains. Experiments were performed once in triplicate for each strain. Bars indicate average with respective standard deviation. Samples **3** and **11** were only tested on gram-positive strains due to sample availability.

2.4. Assessment of test compounds against HIV-1 reverse transcriptase

Previously undescribed compounds and extracts were found to be inactive when assessed for their ability to inhibit HIV-1 reverse transcriptase and they were inactive at 50 mM against FM-55 M1 melanoma cells.

3. Concluding remarks

Nineteen compounds have been isolated and characterised from the Kenyan *Croton schefflera.* Of these compounds, the bark yielded six previously undescribed compounds and four known compounds, while the leaves yielded six known compounds. The structures of the compounds were determined using spectroscopic and spectrometric methods, NMR, IR, UV, polarimetry, ECD, HRESIMS, and GC-MS. Compounds **1**, **4**, **5**, **6**, **7**, **10**, **12** and **19** increased proliferation of serum starved dermal fibroblast cells at a concentration of 100 nM and may have future application for wound healing purposes.

4. Experimental section

4.1. General experimental procedures

NMR spectra were obtained using a Bruker ADVANCE III 400 MHz spectrometer. All spectra were recorded in deuterated chloroform ($CDCl_3$) and calibrated at a chemical shift of δ 7.26 ppm in the ^{1}H NMR spectrum and δ 77.23 ppm in the ^{13}C NMR spectrum. The presence of hydroxy groups was confirmed by recording spectra in deuterated DMSO calibrated to δ 2.50 ppm in the ^{1}H and at δ 39.51 ppm in the ^{13}C NMR spectra. The NMR spectra were processed using the Brucker NMR Topspin software 4.1.3.

HRMS was obtained using a Vanquish UHPLC system connected to a 100 Hz photodiode array detector (PDA), an Orbitrap Fusion Tribrid (Thermo Scientific) high-resolution tandem mass spectrometer. Chromatographic separation (5 µL) was carried out on a C_{18} column Luna (150 mm × 3 mm i.d., 3 µm, Phenomenex, Torrance, CA, USA) operating a mobile phase gradient of 0:90:10 to 90:0:10 (MeOH (A): H_2O (C): CH_3CN + 1% formic acid (D)) over 60 min. Thus, 90% A was held for 10 min and returned to the start conditions for up to 5 min at 30 °C (flow rate: 400 µL/min). UV detection was effectuated between 210 and 550 nm. Mass spectrometry detection was compiled in both the positive and negative ionisation modes with the full scan and data dependent MS^2 and MS^3 acquisition modes. Samples were dissolved in methanol for analysis.

IR spectra were obtained using a Thermo Scientific Nicolet IS5 FT-NIR Spectrometer at Kingston University or a PerkinElmer Universal ATR Accessory FT-NIR Spectrometer at Jodrell Laboratory, Kew Gardens.

UV–Visible spectra were obtained using an Agilent spectrophotometer. The solvent used was methanol and concentrations ranged from 0.0056 to 0.47 mg/mL.

Optical rotation was measured using a ADP220 Bellingham + Stanley Ltd. The concentrations were determined to calculate the specific rotation ($[\alpha]_\lambda^T = (\alpha_\lambda^T)/l \times c$). The temperature was 20–25 °C, the wavelength λ in the sodium D-line, the path length l = 0.1 dm, and the concentration in g/100 mL. The ECD spectra were measured on an Applied Photophysics Chirascan CD spectrometer at the Department of Chemistry, University of Surrey, Guildford, using a 1 mm cell at room temperature. The pure compounds were diluted in acetonitrile (CH_3CN).

TLC was done using Merch KGaA, 64271 Silica gel 60 F_{254} Aluminium backed plates (20 × 20 cm) obtained from Merck, Poole Dorset. Purity of compounds was determined by NMR (Supplementary data S2).

4.2. Plant material

Croton scheffleri Pax LMPM 2019/002 (500 g) was collected from Kibwezi, Voi Kibwezi, and Chyulu. The plant was identified by the taxonomist of the Department of Botany, University of Nairobi.

4.3. Extraction and isolation

The collected bark and leaves of *C. scheffleri* were kept in the dark and dried to avoid the decomposition of its phytochemical components under sunlight. The dried bark and leaves were powdered and separately immersed in dichloromethane (DCM) for 48 h at room temperature, followed by methanol for 48 h. Each extract was filtered and then concentrated using a rotary evaporator. The evaporated extracts were weighed and stored at +4 °C until further analysis.

The dichloromethane extract (3.22 g) of the bark of *C. scheffleri* yielded seven compounds, six had not been described previously, and one was a known clerodane, crotodictyo C (**5**), reported by Munissi et al. (2020) The previously undescribed compounds **2, 6** and **7**, were identified as clerodanes; while compounds **8, 11**, and **12** were sesquiterpenes (Fig. 1). The methanol extract of the bark of the *C. scheffleri* (6.35 g) yielded five compounds, four were previously undescribed and one was a known indole alkaloid (**13**) previously isolated by Aderogba et al. (2013) from *Croton menyharthii*. The previously undescribed compounds were two clerodanes **1** and **4** and two sesquiterpenes **9** and **10** (Fig. 1). The DCM extract of the leaves (9.84 g) yielded six known compounds, Ayanin (**14**) (Yuan et al., 2017), pheophytin a (**15**) (Kurihara et al., 2014), ferulic acid (**16**) (Jayaprakasam et al., 2006), 1,3,4-trihydroxybenzene (**17**) (Li et al., 2023), sitosterol (**18**) (Lizazman et al., 2023), and podosterol (**19**) (Liu et al., 2017).

The DCM extract of the bark of *C. scheffleri* (3.22 g) was fractionated using column chromatography (3 cm diameter, 45 cm height) with silica gel Merch 9385 as the stationary phase and 10% EtOAC: 90% DCM as the mobile phase. Increasing the EtOAc concentration resulted in 111 fractions. The vials containing similar compounds were combined after TLC analysis of the fractions and the proton ^{1}H NMR spectrum. The details for subsequent columns are shown in supplementary information (S1).

The fraction 51–55 (145 mg) yielded two pure compounds **8** (13.9 mg) and **11** (7.3 mg), and the fraction 91 (78.4 mg), which was

separated from the previous fractions 51–55, yielded two compounds, **3** (13.9 mg) and **7** (26.1 mg). While the fraction 4–7 (252.9 mg) yielded compound **12** (18.6 mg). Fractions 8–12 (48.2 mg) yielded compound **5** (17.2 mg). Sephadex LH-20 stationary phase was used to separate the fractions 22–26 (249.5 mg), which yielded compound **4** (16.9 mg), and the fraction 34–50 (394.9 mg) yielded compound **2** (92.0 mg).

The methanol extract of the bark of *C. scheffleri* Pax. (6.35 g) was fractionated using flash column chromatography (3 cm diameter, 45 cm height), using the stationary phase 60 40–63 μM silica gel, and the gradient elution mobile phase starting from 50% Hexane: 50% EtOAC, with increasing concentration of EtOAc until a final wash with methanol to give 1245 fractions. This yielded the compound **1** (17.5 mg). Compound **3** (13.1 mg) was obtained by further purification using flash chromatography (Biotage) and the Biotage® SNAP cartridge KP-SIL 100 g as a stationary phase (80% Hexane: 20% EtOAC). Further column chromatography with 60 40–63 μM silica gel (70% Hexane: 30% EtOAC, increasing EtOAc concentration), yielded compounds **6** (6.1 mg), **9** (6.0 mg), **10** (3.4 mg) and the known indole alkaloid **13** (Aderogba et al., 2013) (10.0 mg).

The DCM extract of the leaves of *C. sheffleri* was fractionated over silica gel (60 40–63 μM) starting with a mobile phase of 60% hexane, 20% DCM, 20% EtOAc, increasing the concentration of EtOAc. Further fractionation using silica gel (60 40–63 μM) and 20% EtOAc:80% hexane lead to the isolation of, Ayanin (**14**), ferulic acid (**16**), 1,3,4-trihydroxybenzene (**17**), sitosterol (**18**) and podosterol (**19**), with pheophytin a (**15**) requiring a further column using Sephadex LH20 (1:1 DCM: MeOH).

4.4. Compound characterisation

Crotoschefferiolide A **(1)** Yellow gum, (17.5 mg); $[\alpha]^{25}{}_{D}$ −0.06 (c 1.71, MeOH); UV λ_{max} (MeOH) (logε) 254 (3.04); IR (NaCl) ν_{max} (cm^{-1}): 3459, 3016, 2958, 1771, 1679; ^{1}H and ^{13}C NMR data are given in Tables 1 and 2; HRESIMS *m/z* 375.1433 $[M+H]^+$ (calcd, m/z 375.1444); ECD (CH_3CN) λ (≤ 1 mg/mL) (Δε) 215 nm (+2.42), 239 nm (−4.81).

Crotoschefferiolide B **(2)** Colourless Oil, (111.0 mg); $[\alpha]_D^{24.1}$ +0.23 (c 0.44, MeOH); UV λ_{max} (MeOH) (logε) 255 (3.45); IR (ATR) ν_{max} (cm-^{1}): 3135, 2955, 1777, 1742, 1721, 1672, 1158; ^{1}H and ^{13}C NMR data are given in Tables 1 and 2; HRESIMS m/z 389.1594 (calcd. for $[M+H]^+$, m/z 389.1556); ECD (CH_3CN) λ (≤ 1 mg/mL) (Δε) 217 nm (+7.9).

Crotoschefferiolide C **(3)** Colourless Oil, (0.4 mg); $[\alpha]_D^{24.1}$ +5.00 (c 0.02, MeOH); IR (ATR) ν_{max} (cm-^{1}): 3333, 2917, 2849, 1634, 1063 ^{1}H and ^{13}CNMR data are given in Tables 1 and 2; HRESIMS *m/z* 389.1594 $[M-1]^+$ (calcd. For $[M-1]^+$, *m/z* 389.1236); ECD (CH_3CN) λ (≤ 1 mg/mL) (Δε) 218 nm (+16.12).

Crotoschefferiolide D **(4)** White powder, (1.1 mg); $[\alpha]^{25}{}_{D}$ +0.25 (c 1.2, MeOH); UV λ_{max} (MeOH) (logε) 213 (4.03), 254 (3.67); IR (ATR) ν_{max} (cm-^{1}): 3364, 1790, 1634, 1538, 1204; ^{1}H and ^{13}C NMR data are given in Tables 1 and 2; HRESIMS *m/z* 489.2119 $[M+1]^+$ (calcd. for $[M+1]^+$, *m/z* 489.2125); ECD (CH_3CN) (≤ 1 mg/mL) (Δε) 200 nm (−0.41), 218 nm (+5.38), 254 nm (−1.21).

Crotoschefferiolide E **(6)** Yellow gum, (6.1 mg); $[\alpha]^{25}{}_{D}$ +0.21 (c 0.47, MeOH); UV λ_{max} (MeOH) (logε) 280 (2.44); IR (NaCl) ν_{max} (cm^{-1}): 3478, 2973, 2933, 1739, 1800, 1761, 1743, 1641, 1376; ^{1}H and ^{13}C NMR data are given in Tables 1 and 2; HRESIMS *m/z* 421.1855 $[M+1]^+$ (calcd $[M+1]^+$, m/z 421.1862); ECD (CH_3CN) λ (≤ 1 mg/mL) (Δε) 224 nm (−1.99), 246 nm (+2.48), 291 nm (−0.13).

Crotoschefferiolide F **(7)** Dark yellow gum, (26.1 mg); $[\alpha]^{24.2}{}_{D}$ −0.09 (c 2.08, MeOH); UV λ_{max} (MeOH) (logε) 263 (2.58); IR (ATR) ν_{max} (cm^{-1}): 2928, 1762, 1725, 1238, 1026; ^{1}H and ^{13}C NMR data are given in Tables 1 and 2; HRESIMS *m/z* 433.1857 $[M+1]^+$ (calcd $[M+1]^+$ 433.1862); ECD (CH_3CN) λ (≤ 1 mg/mL) (Δε) 221 nm (−21.58).

Crotoschefferiune G (8-*epi*-ermiasolide C) **(9)** White powder, (6.0 mg); $[\alpha]^{25}{}_{D}$ +0.43 (c 0.47, MeOH); UV λ_{max} (MeOH) (logε) 220 (3.89); IR (NaCl) ν_{max} (cm^{-1}): 3490, 2931, 2859, 1736, 1681, 1034; ^{1}H and ^{13}C NMR data are given in Table 1 and 2; HRESIMS *m/z* 251.1647 $[M+1]^+$ (calcd$[M+1]^+$, *m/z* 251.1647); ECD (CH_3CN) λ (≤ 1 mg/mL) (Δε) 223 nm (+43.39).

Crotoschefferiune H **(11)** oily pale yellow, (7.3 mg); $[\alpha]^{24.2}{}_{D}$ −0.24 (c 0.42, MeOH); UV λ_{max} (MeOH) (logε) 241 (3.97); IR (NaCl) ν_{max} (cm^{-1}): 3475, 2927, 2856, 1717; ^{1}H and ^{13}C NMR data are given in Tables 1 and 2; HRESIMS *m/z* 237.1851 $[M+1]^+$ (calcd $[M+1]^+$, *m/z* 237.1854); ECD (CH_3CN) λ (≤ 1 mg/mL) 194 nm (−9.54), 247 nm (+1.27), 286 nm (−2.33).

Crotoschefferiune I **(12)** Yellow gum, (18.6 mg); $[\alpha]^{25}{}_{D}$ +0.29 (c 0.35, MeOH); UV λ_{max} (MeOH) (logε) 230 (3.1); IR (NaCl) ν_{max} (cm^{-1}): 3453, 2930, 2856, 1735; ^{1}H and ^{13}C NMR data are given in Tables 1 and 2; HRESIMS *m/z* 217.1585 $[M-5]^+$ (calcd$[M-5]^+$, *m/z* 217.1592); ECD (CH_3CN) λ (≤ 1 mg/mL) 193 nm (+5.20), 202 nm (+6.22), 234 nm (+3.74), 254 nm (+3.35).

4.5. Computational methods

4.5.1. ECD analysis

The calculated ECD spectra of previously undescribed compounds were performed as previously reported (Aldhaher et al., 2017). Systematic conformational searches were performed firstly using MOE software and conformers under 3.0 kcal/mol were optimized using the DFT method at the B3LYP/6-31+G(d) level (Gaussian 09) (Frisch et al., 2016) ECD spectra were simulated using Time Dependant Density Functional Theory (TDDFT) at the CAM-B3LYP/6-31+G(d) level of theory. A polarizable continuum model (IEFPCM, solvent: acetonitrile) was applied to mimic the effects of the solvent used in the experimental ECD spectra. The ECD curves were extracted using SpecDis 1.61 software (Bruhn et al., 2014). The overall ECD curves of all the compounds were weighted by Boltzmann distribution after UV correction.

4.6. Biological assays

4.6.1. Stimulation of serum starved human dermal fibroblasts

Human adult dermal fibroblasts (passage number 15) were maintained in a 5% CO_2 environment at 37 °C in DMEM supplemented with L-glutamine, 10% foetal sterile-filtered bovine serum (Gibco) and 1% antibiotic antimycotic. Cells were seeded into transparent 96 well plates (Nunclon Delta Surface) at 1,000 cells per well and allowed to attach overnight. The cells were then serum starved for 24 h at 37 °C by twice replacing the medium with no serum medium to ensure removal of residual serum. Test compounds (all 10 mM in DMSO), were serially diluted in DMEM 10% FBS using three sequential ten-fold dilution steps. Compounds were then added in a 1/10 dilution step to 96 well plates pre-seeded with cells, thereby achieving final test concentrations of 100 μM, 10 μM, 1 μM and 0.1 μM and a final serum concentration of 1%. No compound control wells containing cells in culture medium with DMSO concentrations corresponding to each dilution step or water were included along with positive control wells containing recombinant TGF-β (Peprotech) solubilised in water. Cells were counted using a Tecan SparkCyto imaging plate reader set to automated cell counting mode. Cells counts were performed immediately after adding compounds and again after 72 h incubation with compounds. Data were analysed using GraphPad Prism software. Pair-wise comparisons were carried out for each treatment versus the corresponding solvent vehicle control (DMSO or water) using a one-way ANOVA correcting for multiple comparisons using a Bonferroni test.

4.6.2. Antibacterial activity

Bacterial strains *Enterococcus faecalis* ATCC 29212, *Escherichia coli* ATCC 25922, *Pseudomonas aeruginosa* ATCC 27853 and *Staphylococcus aureus* ATCC 29213 were obtained from Microbiologics Inc. (St. Cloud, Minnesota, USA). Strains were stored at −80 °C and working cultures maintained on Mueller-Hinton Agar (MHA, Lab M Limited) plates and stored at 2–8 °C. To determine the antibacterial activity of extracts and pure compounds samples were resuspended in 100% DMSO at 200 mg/

mL and 10 mg/mL, respectively. Antibacterial screenings were carried out based on the broth microdilution assays in 96-well plates following the Clinical and Laboratory Standards Institute guidelines (CLSI, 2008). Briefly, bacterial cultures were initiated on Mueller Hinton agar plates, and prior to the assays bacterial suspension was diluted in cation-adjusted Mueller Hinton broth (CAMHB) to obtain a final inoculum of 5×10^5 CFU/mL. An equal volume of bacterial suspension and samples' solution, diluted into assay media (CAMHB) were mixed on the plate and incubated for 24 h at 37 °C. Absorbance values measured at 620 nm were used for evaluating the antimicrobial effects of extracts by comparing to untreated controls and expressed as percentage inhibition of growth. Visual assessments were also taken into consideration due to the intrinsic colour and precipitation of certain extracts, which can influence absorbance values. Screenings against all bacterial strains mentioned above were performed with pure compounds at 50 μg/mL and extracts at 1 mg/mL, and growth inhibitions calculated. Assays were performed once in triplicate. Ciprofloxacin (ICN Biomedicals) was used as positive control on every assay plate at MIC (previously determined in our laboratory) for each bacterium, i.e., *E. coli* (0.02 μg/mL), *E. faecalis* and *P. aeruginosa* (1 μg/mL) and *S. aureus* ATCC 29213 (0.5 μg/mL).

4.6.3. HIV-1 reverse transcriptase inhibition determination

The HIV-1 reverse transcriptase inhibition assay was conducted *in vitro* using the EnzChek® Reverse transcriptase assay kit (E-22064) provided by Molecular Probes (Eugene, OR, USA), following the manufacturer's instructions. Reverse transcriptase was purchased from Promega (Madison, WI, USA) (GoScript™ Reverse Transcriptase: catalogue number A5004) and the enzyme dilution buffer from Thermo Fisher (Waltham, MA, USA) (catalogue number B19). Briefly, the EnzChek® RT kit caters to 1000 assays. Assays were performed in increments of 96 using a 96-well microtiter plate. GoScript™ RT was supplied at a concentration of 160 u/μL, but was diluted to 53.3 u/μL in enzyme dilution buffer and frozen as 10 aliquots in volumes of 150 μL at −80 °C. A preliminary run was conducted using titrants of the RT to determine the ideal starting concentration, using a ladder with a starting concentration of 26.7 u/μL. A final enzyme concentration of 1.1 u/μL was used, so frozen stock was diluted to 3.3 u/μL in enzyme dilution buffer as the aliquot concentration to give the final concentration of 1.1 u/μL after the reactants were combined. The assay was initiated by annealing of the template and primer. A volume of 5 μL of the poly(A) ribonucleotide template was combined with 5 μL of oligo $d(t)_{16}$ primer and allowed to anneal for an hour at room temperature. After annealing, the 10 μL volume of template/primer was diluted by adding 1.99 mL of polymerisation buffer. The resulting solution was used as the reaction mixture. The reaction was commenced by combining 20 μL of reaction mixture and 20 μL of treatment, and thereafter adding 20 μL of enzyme at 3.4 u/μL. The reaction was completed after 1 h at 25 °C and terminated with the addition of 30 μL of 15 mM EDTA. Results were determined by adding 180 μL of PicoGreen® dsDNA quantitation reagent solution to the wells and allowing 5 min to pass before reading fluorescence intensity, using 480 nm as excitation wavelength and 520 nm for emission wavelength. The fluorescence value of the control (wells with no enzyme) was subtracted from that of each of the samples. The results are reported as concentration of treatment to give 50% enzyme inhibition (EC_{50}). The compounds tested were prepared by dissolving to a concentration of 20 mg/mL in dimethyl sulfoxide and diluting in nuclease free water to three times the desired starting concentration. A starting concentration of 50 μg/mL was used, so aliquot concentration was 150 μg/mL. All samples were assayed in triplicate and the averages are provided as results.

CRediT authorship contribution statement

Mona Diri: Writing – review & editing, Writing – original draft, Investigation, Data curation. **Moses K. Langat:** Writing – review & editing, Writing – original draft, Supervision, Data curation, Conceptualization. **Eduard Mas-Claret:** Writing – review & editing, Writing – original draft, Investigation, Data curation. **Thomas A.K. Prescott:** Writing – review & editing, Writing – original draft, Methodology, Investigation, Formal analysis, Data curation. **Cristina D. Cruz:** Writing – review & editing, Writing – original draft, Methodology, Investigation, Data curation. **Päivi Tammela:** Writing – review & editing, Supervision, Data curation, Conceptualization. **Sianne Schwikkard:** Writing – review & editing, Writing – original draft, Supervision, Data curation, Conceptualization.

Declaration of competing interest

The authors declare the following financial interests/personal relationships which may be considered as potential competing interests: Tammela reports financial support was provided by EU Framework Programme for Research and Innovation Euratom. If there are other authors, they declare that they have no known competing financial interests or personal relationships that could have appeared to influence the work reported in this paper. This is financial support for the project, no competing interests.

Acknowledgements

The authors Cristina D. Cruz and Päivi Tammela would like to thank the European Union's Horizon 2020 research and innovation programme grant agreement No 951883 (SPRINGBOARD) for funding. We also thank Patrick Mutiso Chalo for collection and identification of the plant.

Appendix A. Supplementary data

Supplementary data to this article can be found online at https://doi.org/10.1016/j.phytochem.2025.114460.

Data availability

Data will be made available on request.

References

Aderogba, M.A., Ndhlala, A.R., Rengasamy, K.R.R., Van Staden, J., 2013. Antimicrobial and selected in vitro enzyme inhibitory effects of leaf extracts, flavonols and indole alkaloids isolated from *Croton menyharthii*. Molecules 18, 12633–12644. https://doi.org/10.3390/molecules181012633.

Aldhaher, A., Langat, M., Ndunda, B., Chirchir, D., Midiwo, J.O., Njue, A., Schwikkard, S., Carew, M., Mulholland, D., 2017. Diterpenoids from the roots of *Croton dichogamus* Pax. Phytochemistry 144, 1–8. https://doi.org/10.1016/j.phytochem.2017.08.014.

Bruhn, T., Schaumlöffel, A., Hemberger, Y., Bringmann, G., 2014. SpecDis.

CLSI, 2008. Reference Method for Broth Dilution Antifungal Susceptibility Testing of Yeasts: Approved Standard, third ed. M27-A3. Clinical and Laboratory Standards Institute, Wayne, PA.

Fern, K., 2021. Useful Tropical Plants Database, tropical.theferns.Info.

Frisch, M.J., Trucks, G.W., Schlegel, H.B., Scuseria, G.E., Robb, M.A., Cheeseman, J.R., Scalmani, G., Barone, V., Petersson, G.A., Nakatsuji, H., Li, X., Caricato, M., Marenich, A.V., Bloino, J., Janesko, B.G., Gomperts, R., Mennucci, B., Hratchian, H. P., Ortiz, J.V., Izmaylov, A.F., Sonnenberg, J.L., Williams, Ding, F., Lipparini, F., Egidi, F., Goings, J., Peng, B., Petrone, A., Henderson, T., Ranasinghe, D., Zakrzewski, V.G., Gao, J., Rega, N., Zheng, G., Liang, W., Hada, M., Ehara, M., Toyota, K., Fukuda, R., Hasegawa, J., Ishida, M., Nakajima, T., Honda, Y., Kitao, O., Nakai, H., Vreven, T., Throssell, K., Montgomery, Jr.J.A., Peralta, J.E., Ogliaro, F., Bearpark, M.J., Heyd, J.J., Brothers, E.N., Kudin, K.N., Staroverov, V.N., Keith, T.A., Kobayashi, R., Normand, J., Raghavachari, K., Rendell, A.P., Burant, J.C., Iyengar, S. S., Tomasi, J., Cossi, M., Millam, J.M., Klene, M., Adamo, C., Cammi, R., Ochterski, J. W., Martin, R.L., Morokuma, K., Farkas, O., Foresman, J.B., Fox, 2016. D. J. Gaussian 16 Rev. C.01. https://gaussian.com/citation/.

Guetchueng, S.T., Nahar, L., Ritchie, K.J., Ismail, F.M.D., Evans, A.R., Sarker, S.D., 2018. *Ent*-clerodane diterpenes from the bark of *Croton oligandrus* Pierre Ex Hutch. And assessment of their cytotoxicity against human cancer cell lines. Molecules 23, 410. https://doi.org/10.3390/molecules23020410.

Isyaka, S.M., Langat, M.K., Mas-Claret, E., Mbala, B.M., Mvingu, B.K., Mulholland, D.A., 2020. *Ent*-abietane and *ent*-pimarane diterpenoids from *Croton mubango* (Euphorbiaceae). Phytochemistry 170, 112217. https://doi.org/10.1016/j.phytochem.2019.112217.

Jayaprakasam, B., Vanisree, M., Zhang, Y., Dewitt, D.L., Nair, M.G., 2006. Impact of alkyl esters of caffeic and ferulic acids on tumor cell proliferation, cyclooxygenase enzyme, and lipid peroxidation. J. Agric. Food Chem. 54, 5375–5381. https://doi.org/10.1021/jf060899p.

Kawakami, S., Inagaki, M., Matsunami, K., Otsuka, H., Kawahata, M., Yamaguchi, K., 2016. Crotofolane-type diterpenoids, crotocascarins L–Q, and a rearranged crotofolane-type diterpenoid, neocrotocascarin, from the stems of *Croton cascarilloides*. Chem. Pharm. Bull. (Tokyo) 64, 1492–1498. https://doi.org/10.1248/cpb.c16-00500.

Kurihara, H., Kagawa, Y., Konno, R., Kim, S.M., Takahashi, K., 2014. Lipoxygenase inhibitors derived from marine macroalgae. Bioorg. Med. Chem. Lett. 24, 1383–1385. https://doi.org/10.1016/j.bmcl.2014.01.046.

Langat, M., Mulholland, D.A., Crouch, N.R., 2008. New diterpenoids from *Croton sylvaticus* and *Croton pseudopulchellus* (Euphorbiaceae) and antiplasmodial screening of *ent*-kaurenoic acid. Planta Med. 74, PB126. https://doi.org/10.1055/s-0028-1084471.

Langat, M.K., Crouch, N.R., Smith, P.J., Mulholland, D.A., 2011. Cembranolides from the leaves of *Croton gratissimus*. J. Nat. Prod. 74, 2349–2355. https://doi.org/10.1021/np2002012.

Langat, M.K., Crouch, N.R., Pohjala, L., Tammela, P., Smith, P.J., Mulholland, D.A., 2012. *Ent*-Kauren-19-Oic acid derivatives from the stem bark of *Croton pseudopulchellus* Pax. Phytochem. Lett. 5, 414–418. https://doi.org/10.1016/j.phytol.2012.03.002.

Langat, M.K., Crouch, N., Ndunda, B., Midiwo, J.O., Aldhaher, A., Alqahtani, A., Mulholland, D.A., 2016. The chemistry of African Croton species. Planta Med. 82 (S 01), P384. https://doi.org/10.1055/s-0036-1596495.

Langat, M.K., Crouch, N.R., Nuzillard, J.-M., Mulholland, D.A., 2018. Pseudopulchellol: a unique sesquiterpene-monoterpene derived C-25 terpenoid from the leaves of *Croton pseudopulchellus* Pax (Euphorbiaceae). Phytochem. Lett. 23, 38–40. https://doi.org/10.1016/j.phytol.2017.11.008.

Langat, M.K., Ndunda, B.M., Salter, C., Odusina, B.O., Isyaka, S.M., Mas-Claret, E., Onocha, P.A., Midiwo, J.O., Nuzillard, J.-M., Mulholland, D.A., 2020a. Diterpenoids from the stem bark of *Croton megalocarpoides* Friis & M. G. Gilbert. Phytochem. Lett. 39, 1–7. https://doi.org/10.1016/j.phytol.2020.07.003.

Langat, M.K., Djuidje, E.F.K., Ndunda, B.M., Isyaka, S.M., Dolan, N.S., Ettridge, G.D., Whitmore, H., Lopez, I., Alqahtani, A.M., Atiku, I., Lobe, J.S., Mas-Claret, E., Crouch, N.R., Midiwo, J.O., Mulholland, D.A., Kamdem, A.F.W., 2020b. The phytochemical investigation of five African *Croton* species: *Croton oligandrus, Croton megalocarpus, Croton menyharthii, Croton rivularis* and *Croton megalobotrys*. Phytochem. Lett. 40, 148–155. https://doi.org/10.1016/j.phytol.2020.09.020.

Lebwohl, M., Swanson, N., Anderson, Lawrence L., Melgaard, A., Xu, Z., Berman, B., 2012. Ingenol mebutate gel for actinic keratosis. N. Engl. J. Med. 366, 1010–1019. https://doi.org/10.1056/NEJMoa1111170.

Li, S.C., Jin, Y.J., Xue, X., Li, J., Xu, G.H., 2023. Chemical constituents from the bark of *Betula platyphylla*. Chem. Nat. Compd. 59, 190–192. https://doi.org/10.1007/s10600-023-03951-7.

Liu, J., Gao, Z.-H., Wu, J.-C., Chen, Y.-G., 2017. A new 5(6→7)Abeo-sterol from *Podocarpus fleuryi*. J. Asian Nat. Prod. Res. 19, 1022–1027. https://doi.org/10.1080/10286020.2017.1283309.

Lizazman, M.A., Jong, V.Y.M., Chua, P., Lim, W.K., Karunakaran, T., 2023. Phytochemicals from *Calophyllum canum* Hook f. Ex T. Anderson and their neuroprotective effects. Nat. Prod. Res. 37, 2043–2048. https://doi.org/10.1080/14786419.2022.2116021.

Lovett, J.C., 1993. Eastern Arc moist forest flora. In: Biogeography and Ecology of the Rain Forests of Eastern Africa. Cambridge University Press, pp. 33–56.

Matara, D., Nguta, J., Musila, F., Ole-Mapenay, I., Ali, H., Omambia, V., 2021. Botanical description, ethnomedicinal uses, phytochemistry and pharmacological effects of *Croton dichogamus* Pax (Euphorbiaceae). J. Phytopharm. 10, 42–47. https://doi.org/10.31254/phyto.2021.10109.

Moremi, M.P., Makolo, F., Viljoen, A.M., Kamatou, G.P., 2021. A review of biological activities and phytochemistry of six ethnomedicinally important South African *Croton* species. J. Ethnopharmacol. 280, 114416. https://doi.org/10.1016/j.jep.2021.114416.

Moses, R.L., Boyle, G.M., Howard-Jones, R.A., Errington, R.J., Johns, J.P., Gordon, V., Reddell, P., Steadman, R., Moseley, R., 2020a. Novel epoxy-tiglianes stimulate skin keratinocyte wound healing responses and Re-epithelialization via protein kinase C activation. Biochem. Pharmacol. 178, 114048. https://doi.org/10.1016/j.bcp.2020.114048.

Moses, R.L., Dally, J., Lundy, F.T., Langat, M., Kiapranis, R., Tsolaki, A.G., Moseley, R., Prescott, T.A.K., 2020b. Lepiniopsis ternatensis sap stimulates fibroblast proliferation and down regulates macrophage TNF-α secretion. Fitoterapia 141, 104478. https://doi.org/10.1016/j.fitote.2020.104478.

Moses, R.L., Prescott, T.A.K., Mas-Claret, E., Steadman, R., Moseley, R., Sloan, A.J., 2023. Evidence for natural products as alternative wound-healing therapies. Biomolecules 13, 444. https://doi.org/10.3390/biom13030444.

Mulholland, D.A., Langat, M.K., Crouch, N.R., Coley, H.M., Mutambi, E.M., Nuzillard, J.-M., 2010. Cembranolides from the stem bark of the southern African medicinal plant, *Croton gratissimus* (Euphorbiaceae). Phytochemistry 71, 1381–1386. https://doi.org/10.1016/j.phytochem.2010.05.014.

Munissi, J.J.E., Isyaka, S.M., Mas-Claret, E., Brabner, M., Langat, M.K., Nyandoro, S.S., Mulholland, D.A., 2020. *Ent*-clerodane and *ent*-trachylobane diterpenoids from *Croton dictyophlebodes*. Phytochemistry 179, 112487. https://doi.org/10.1016/j.phytochem.2020.112487.

Ndunda, B., Langat, M.K., Wanjohi, J.M., Midiwo, J.O., Kerubo, L.O., 2013. Alienusolin, a new 4α-deoxyphorbol ester derivative, and Crotonimide C, a new glutarimide alkaloid from the Kenyan *Croton alienus*. Planta Med. 79, 1762–1766. https://doi.org/10.1055/s-0033-351044.

Ndunda, B., Langat, M.K., Midiwo, J.O., Omosa, L.K., 2015. Diterpenoid derivatives of Kenyan *Croton sylvaticus*. Nat. Prod. Commun. 10, 1934578X1501000403. https://doi.org/10.1177/1934578X1501000403.

Ndunda, B., Langat, M.K., Mulholland, D.A., Eastman, H., Jacob, M.R., Khan, S.I., Walker, L.A., Muhammad, I., Kerubo, L.O., Midiwo, J.O., 2016. New *ent*-clerodane and abietane diterpenoids from the roots of Kenyan *Croton megalocarpoides* Friis & M. G. Gilbert. Planta Med. 82, 1079–1086. https://doi.org/10.1055/s-0042-108857.

Ngumbau, V.M., Nyange, M., Wei, N., van Ee, B.W., Berry, P.E., Malombe, I., Hu, G.-W., Wang, Q.-F., 2020. A new species of *Croton* (Euphorbiaceae) from a Madagascan lineage discovered in coastal Kenya. Syst. Bot. 45, 242–248. https://doi.org/10.1600/036364420X15862837791294.

Prescott, T.A.K., Kiapranis, R., Maciver, S.K., 2012. Comparative ethnobotany and in-the-field antibacterial testing of medicinal plants used by the Bulu and Inland Kaulong of Papua New Guinea. J. Ethnopharmacol. 139, 497–503. https://doi.org/10.1016/j.jep.2011.09.058.

Rayanil, K., Limpanawisut, S., Tuntiwachwuttikul, P., 2013. *Ent*-pimarane and *ent*-trachylobane diterpenoids from *Mitrephora alba* and their cytotoxicity against three human cancer cell lines. Phytochemistry 89, 125–130. https://doi.org/10.1016/j.phytochem.2013.01.012.

Reddell, P., De Ridder, T.R., Morton, J.M., Jones, P.D., Campbell, J.E., Brown, G., Johannes, C.M., Schmidt, P.F., Gordon, V., 2021. Wound Formation, wound size, and progression of wound healing after intratumoral treatment of mast cell tumors in dogs with tigilanol tiglate. J. Vet. Intern. Med. 35, 430–441. https://doi.org/10.1111/jvim.16009.

Sadgrove, N.J., Madeley, L.G., Wyk, B.-E.V., 2019. Volatiles from African species of *Croton* (Euphorbiaceae), including new diterpenes in essential oil from *Croton gratissimus*. Heliyon 5, e02677. https://doi.org/10.1016/j.heliyon.2019.e02677.

Terefe, E.M., Okalebo, F.A., Derese, S., Muriuki, J., Rotich, W., Mas-Claret, E., Sadgrove, N., Padilla-González, G.F., Prescott, T.A.K., Siddique, H., Langat, M.K., 2022a. Constituents of *Croton megalocarpus* with potential anti-HIV activity. J. Nat. Prod. 85, 1861–1866. https://doi.org/10.1021/acs.jnatprod.1c01013.

Terefe, E.M., Okalebo, F.A., Derese, S., Langat, M.K., Mas-Claret, E., Qureshi, K.A., Jaremko, M., Muriuki, J., 2022b. Anti-HIV ermiasolides from *Croton megalocarpus*. Molecules 27, 7040. https://doi.org/10.3390/molecules27207040.

Terefe, E.M., Okalebo, F.A., Derese, S., Muriuki, J., Mas-Claret, E., Langat, M.K., 2023. Anti-HIV crotocascarin ω from Kenyan *Croton dichogamus*. Nat. Prod. Res. 37, 2809–2816. https://doi.org/10.1080/14786419.2022.2134998.

Wall, I.B., Moseley, R., Baird, D.M., Kipling, D., Giles, P., Laffafian, I., Price, P.E., Thomas, D.W., Stephens, P., 2008. Fibroblast dysfunction is a key factor in the non-healing of chronic venous leg ulcers. J. Invest. Dermatol. 128, 2526–2540. https://doi.org/10.1038/jid.2008.114.

Xu, W.-H., Liu, W.-Y., Liang, Q., 2018. Chemical constituents from *Croton* species and their biological activities. Molecules 23, 2333. https://doi.org/10.3390/molecules23092333.

Yamakawa, S., Hayashida, K., 2019. Advances in surgical applications of growth factors for wound healing. Burn Trauma 7, 10. https://doi.org/10.1186/s41038-019-0148-1.

Yang, L., Li, L., Huang, S., Pu, J., Zhao, Y., Ma, Y., Chen, J., Leng, C., Tao, Z., Sun, H., 2011. Anti-hepatitis B virus and cytotoxic diterpenoids from *Isodon lophanthoides* var. *Gerardianus*. Chem. Pharm. Bull. (Tokyo) 59, 1102–1105. https://doi.org/10.1248/cpb.59.1102.

Yuan, Z., Luan, G., Wang, Z., Hao, X., Li, J., Suo, Y., Li, G., Wang, H., 2017. Flavonoids from *Potentilla parvifolia* Fisch. and their neuroprotective effects in human neuroblastoma SH-SY5Y cells *in vitro*. Chem. Biodivers. 14, e1600487. https://doi.org/10.1002/cbdv.201600487.